NAVAL FACILITIES ENGINEERING SERVICE CENTER
Port Hueneme, California 93043-4370

TECHNICAL REPORT
TR-2215-SHR

SALT-FOG ACCELERATED TESTING OF GLASS FIBER REINFORCED POLYMER COMPOSITES

by Arsenio Caceres (University of Puerto Rico),
Robert M. Jamond, Theresa A. Hoffard, L. Javier Malvar (NFESC)

December 2002

REPORT DOCUMENTATION PAGE

Form Approved
OMB No. 0704-0188

1. AGENCY USE ONLY (Leave blank)	2. REPORT DATE	3. REPORT TYPE AND DATES COVERED
	December 2002	Final (FY 01)

4. TITLE AND SUBTITLE
Salt-Fog Accelerated Testing of Glass Fiber Reinforced Polymer Composites

5. FUNDING NUMBERS
N0001401WX20217

6. AUTHOR(S)
A. Caceres, R.M. Jamond, T.A. Hoffard, L.J. Malvar

7. PERFORMING ORGANIZATION NAME(S) AND ADDRESS(ES)
Naval Facilities Engineering Service Center
1100 23rd Avenue
Port Hueneme, CA 93043-4370

8. PERFORMING ORGANIZATION REPORT NUMBER
TR-2215-SHR

9. SPONSORING/MONITORING AGENCY NAME(S) AND ADDRESS(ES)
Office of Naval Research
Ballston Centre Tower One
800 North Quincy Street
Arlington, VA 22217-5660

10. SPONSORING/MONITORING AGENCY
ONR

11. SUPPLEMENTARY NOTES

12a. DISTRIBUTION/AVAILABILITY STATEMENT
Approved for public release, distribution unlimited

12b. DISTRIBUTION CODE

13. ABSTRACT (Maximum 200 words)

The objective of this project was to determine the durability under accelerated salt-fog exposure of six commercially available composites. These composites included glass-reinforced vinylesters, polyesters, phenolics, and an epoxy. Durability was measured mainly in terms of the loss of elastic modulus and flexural strength after exposure. In order to accelerate aging, the specimens were subjected to temperatures of 95°F (35°C), 120°F (49°C), and 160°F (71°C) for one, two and three months each while exposed to a salt-fog spray. A previous project had determined that among the common marine exposures, salt-fog was a major cause for degradation of composites used in the retrofit of the Navy's waterfront infrastructure. Flexural tests were performed, along with dynamic mechanic analyses and scanning electron microscopy. Once the aging effects were determined, a time-temperature superposition analysis was performed in order to extrapolate the results and estimate the degradation over longer time periods. Analysis predictions indicate losses of 35% or more in flexural strength over a 5-year period. To enable predictions beyond 5 years, additional and longer lasting testing would be necessary. Suggestions were made on how to introduce these findings in the design of composite material structures.

14. SUBJECT TERMS	15. NUMBER OF PAGES
GFRP, fiber reinforced polymer, glass fibers, durability, salt fog, accelerated exposure.	53
	16. PRICE CODE

17. SECURITY CLASSIFICATION OF REPORT	18. SECURITY CLASSIFICATION OF THIS PAGE	19. SECURITY CLASSIFICATION OF ABSTRACT	20. LIMITATION OF ABSTRACT
U	U	U	U

NSN 7540-01-280-5500

Standard Form 298 (Rev. 2-89)
Prescribed by ANSI Std Z39-18
298-102

EXECUTIVE SUMMARY

The objective of this project was to determine the durability under accelerated salt-fog exposure of six commercially available composites. These composites included glass-reinforced vinylesters, polyesters, phenolics, and an epoxy. Durability was measured mainly in terms of the loss of elastic modulus and flexural strength after exposure. In order to accelerate aging, the specimens were subjected to temperatures of 95°F (35°C), 120°F (49°C), and 160°F (71°C) for one, two and three months each while exposed to a salt-fog spray. A previous project had determined that among the common marine exposures, salt-fog was a major cause for degradation of composites used in the retrofit of the Navy's waterfront infrastructure. Flexural tests were performed, along with Dynamic Mechanic Analyses and Scanning Electron Microscopy. Once the aging effects were determined, a time-temperature superposition analysis was performed in order to extrapolate the results and estimate the degradation over longer time periods. Analysis predictions indicate losses of 35% or more in flexural strength over a 5-year period. To enable predictions beyond 5 years, additional and longer lasting testing would be necessary. Suggestions were made on how to introduce these findings in the design of composite material structures.

TABLE OF CONTENTS

1. INTRODUCTION **1**

2. LITERATURE REVIEW **1**

3. BACKGROUND **2**

4. TESTING PROGRAM **2**

4.1. SPECIMENS 2
4.2. APPARATUS 3
4.3. ACCELERATED AGING TEMPERATURE 4
4.4. TESTS PERFORMED 5

5. DEGRADATION MECHANISMS **5**

6. ANALYSIS OF RESULTS **8**

6.1. FLEXURAL TESTS 8
6.2. DYNAMIC MECHANIC ANALYSIS 11
6.3. SCANNING ELECTRON MICROSCOPY 12
6.4. MINIMUM ALLOWABLE VALUES 14

7. CONCLUSIONS **14**

8. ACKNOWLEDGEMENTS **15**

9. REFERENCES **15**

APPENDIX A: MASTER CURVES FOR FLEXURAL STRENGTH AT T = 70º F **A-1**

APPENDIX B: MASTER CURVES FOR STIFFNESS AT T = 70º F **B-1**

APPENDIX C: FLEXURAL TEST CURVES **C-1**

APPENDIX D: AVERAGED DMA CURVES OF EXPOSED VERSUS CONTROL FLEXURAL STORAGE AND LOSS MODULI **D-1**

1. INTRODUCTION

Composite materials are being used in the rehabilitation and repair of Naval structures exposed to the marine environment. The use of composites for rehabilitation presents the following advantages: they possess high tensile strength, they are light, composites can be easily bonded to concrete, and they have superior corrosion resistance when compared to traditional construction materials, such as steel and aluminum. However, in order to evaluate the true cost of a specific type of composite, its durability must also be evaluated. The U.S. Navy waterfront infrastructure is subjected to various environmental exposures, including moisture, salt, hot and cold temperatures, and UV radiation. In a previous project, the Naval Facilities Engineering Service Center (NFESC) studied the effects of laboratory simulated marine climates on the mechanical properties of several commercial composites [1, 2] and found that, of all the previous exposures, seawater immersion and salt-fog exposure caused the greatest deterioration of the flexural and tensile strengths of the composites. In order to address the issue of long-term durability under salt-fog conditions, it was suggested that accelerated testing be conducted on the same fiber reinforced composites [3].

2. LITERATURE REVIEW

Knowledge of long-term behavior of composites is required for safe and economical design. The difficulty in predicting the long-term performance of composites arises from the fact that in laboratory tests only short-time results are often obtained. Therefore it is necessary to extrapolate data from short tests to obtain long-term predictions. Several experimental procedures have been used to accelerate the weathering of composites under a variety of aggressive environments. Most of them are based on increasing the intensity of the weathering agent in the expectation that it will accelerate the aging of the material without changing the degradation mechanism. Porter and Barnes [4] have used high alkaline bath and elevated temperature to accelerate alkaline corrosion of E-glass/vinylester composites. Bank, et al. [5] exposed pultruded glass/vinylester rods to several aggressive conditionings for up to 224 days. These conditions included deionized water with high temperature, ammonium hydroxide solutions, pre-strain, and high humidity. This list does not include accelerated testing performed under creep or fatigue loading. Chajes, et al. [6] studied the effect of freeze/thaw or wet/dry cycles in a calcium chloride solution of composites made with aramid, E-glass, and graphite fibers.

Durability testing of fiber reinforced polymer (FRP) composites is already required by several building codes. For instance, such testing is required for seismic upgrades by the California Department of Transportation (CALTRANS) [7, 8] and the International Conference of Building Officials (ICBO) [9], both of which require exposures to salt water. Such exposures have resulted in material property reduction factors that are included in the various international codes for design with composites for infrastructure applications, in particular in Japan [10],

Canada [11, 12], and the United States [13, 14]. For example in the United States, glass bars in concrete exposed to earth and weather must use an environmental exposure reduction factor of 0.7 [13], and FRP systems under exterior exposure must use a reduction factor of 0.65 [14].

3. BACKGROUND

For the analysis in this project a procedure known as the time-temperature superposition (TTS) equivalence or method of reduced variables, based on the Arrhenius model, was used [3]. The TTS principle has been used extensively for the extrapolation of results in time. The method has been successfully used for failure mechanisms that depend on chemical reactions, diffusion processes, or migration processes. The TTS principle is based on the assumption that the processes involved in molecular relaxation or rearrangements in visco-elastic materials occur at accelerated rates at higher temperatures, and that there is a direct equivalence between time (the frequency of measurement) and temperature. Therefore, the time over which these processes occur can be reduced by conducting the measurement at elevated temperatures and transposing (shifting) the resultant data to lower temperatures. The result of this shifting is a "master curve" where the material property of interest at a specific temperature can be predicted over a broad time scale. The TTS does not, however, take into account the effect of sustained load. Interesting applications are found in stress corrosion of borosilicate glass rods, for E-glass fibers [15], and for zero stress aging of glass fibers embedded in concrete [16]. Recently, Iyer, et al. have used it to model creep and creep-rupture of unidirectional composite laminates with good results [17].

4. TESTING PROGRAM

As mentioned, the testing program is a continuation of a previous one recently completed by NFESC in which seven GFRP specimens were tested under several types of marine exposure [1, 2]. In the current phase, only salt-fog exposure was considered since it was found to result, along with seawater immersion, in the fastest composite deterioration. The time-temperature equivalence principle was used in order to extrapolate the short-term behavior.

4.1. Specimens

Six composites were tested:

- Two glass-reinforced vinylesters (here called I and II): two commercial formulations containing epoxy vinylester made with bisphenol-A and styrene.
- Two glass-reinforced polyesters (here called I and II): two commercial resin formulations made with isophthalic acid, maleic anhydride, and common glycols.

- One glass-reinforced phenolic: commercial resin made with phenol and formaldehyde (product is a waterborne, styrene-free, phenolic resole).
- One glass-reinforced epoxy (epoxy-polyamide): A commercial resin made with bisphenol-A epoxy and aromatic amine curing agents.

The nominal dimensions of each composite piece were 10 x 0.5 x 0.125 in. (254 x 12.5 x 3.2 mm), except for the phenolic, which was thinner (0.093 inch or 2.4 mm). These six pultruded glass reinforced thermoset plastic composites are readily available for use in waterfront applications. The composite strips were all made by one company that purchased the resins and fiberglass matting and prepared 6-inch (152.4 mm) wide pultruded strips. The strips had 7 plies of 3-ounce (85 g) and 2 plies of 0.5-ounce (14.2 g) continuous strand E-glass mat, with 8 plies of 113 yield E-glass rovings for the laminate design of the epoxy, polyester, and vinylester specimens. The glass content of the epoxy, polyester, and vinylester composites was 42.5% by weight. However, the rovings made up 28% of the total glass weight. Rovings were unidirectional and run in the long direction. Continuous strand mat was in random orientation. The stitched mat was a combination of 0º and 90º rovings. The phenolic laminates were different due to the chemical method of preparing phenolics (condensation). Phenolic composite coupons had a 60% glass content by weight. The sheeting was cut into 0.5-inch (12.7-mm) strips in the longitudinal direction and the edges were sealed with a UV veil varnish.

4.2. Apparatus

The salt fog chamber (by Auto Technology) is a 20-ft^3 (0.566-m^3) cyclic corrosion chamber used in the automotive industry for cyclic salt fog, drying and humidity tests, as well as other cyclic tests, following ASTM B 117 [18]. In the salt fog cycle, the salt solution is atomized into a fine mist. Hot, humid air is created by bubbling compressed air (usually at 15 psi or 103.4 KPa) through a tube (bubble tower, or humidifying tower) that is about 3/4 full of hot (usually 118°F/48°C) deionized water (see Figure 1).

Figure 1. Auto Technology salt-fog chamber.

The salt solution is moved from the 60-gallon (0.227 m^3) holding tank to the nozzle by a gravity feed system using a float switch and plastic solenoid. When the hot, humid air and the salt solution mix at the nozzle, the latter is atomized into a corrosive fog. The chamber is usually heated during this cycle at 95°F (35°C) by the chamber heaters. The chamber temperature is set by the user, and controlled by a Programmable Logic Controller. Fog distribution is controlled by the

Uni-Fog dispersion system. The salt solution can be replaced by other solutions to create a corrosive fog with differing properties.

Dynamic mechanic analysis (DMA) testing was performed using a TA Instruments DMA-2980. DMA measures the flexural storage modulus (stiffness) and damping (energy dissipation) properties of materials. A sinusoidal deformation force is applied to a material sample as it sits in a clamped configuration (e.g. three-point bending) inside a furnace. The sample deformation that occurs under the applied force is measured as the furnace cycles through a temperature program input by the operator.

For the composite specimens tested, a three-point bending mode was utilized, conforming to ASTM D 4065 [19] and ASTM D 5023 [20]. Composite strip specimens taken from the salt-fog chamber at specified sampling times were cut into 2.36-in (60-mm) lengths for placement in the DMA clamps. Four replicate samples were tested for each type of composite material and each exposure. The DMA furnace was programmed to heat the sample from 95°F (35°C) to approximately 320°F (160°C), or as required to extend past the glass transition phase of the material. The heating rate was set at 3.6ºF/minute (2ºC/minute). The frequency of the sinusoidal force was set at 1.0 Hz. The flexural storage modulus (E') and the flexural loss modulus (E") were plotted against temperature for each sample. The temperature at the peak of the E" curve is taken to be the glass transition temperature, T_g. Data from the exposed specimens were compared to data of control specimens for each type of composite tested.

Specimens were carefully observed under a scanning electron microscope (SEM) for signs of deterioration along with their corresponding control surfaces. Comparisons were made between the control surfaces and the three-month exposed surfaces in order to appreciate signs of deterioration. The SEM observations can help insure that the same degradation mechanism exists during the 3-month testing, a necessary condition for the TTS to be valid.

4.3. Accelerated Aging Temperature

Each test for a specific temperature was performed over 3 months for a total program duration of 9 months. Given the temperature range (95 to 160°F, or 35 to 71°C) where the chamber can operate, the temperatures used to accelerate aging were:

- 95°F (35°C)
- 120°F (48.9°C)
- 160°F (71.1°C)

These temperatures are below the glass transition temperature of the selected thermosets (see Table 1), thus avoiding the change in the degradation mechanism that may occur at that point. A maximum temperature of 0.8 T_g has been suggested for accelerating the degradation process [21]. Others recommend that accelerating temperatures be kept at least 10 to 15°C below the T_g of the matrix. As a result tests are often conducted at 60°C, 80°C, and sometimes even higher temperatures [21, 22].

Table 1. Glass Transition Temperatures T_g in Degrees Centigrade. (Peak of E" Flexural Loss Modulus Curve)

Specimen	Control	95°F / 3 Month	120°F / 3 Month	160°F / 2 Month
Vinylester I (A)	108.4	106.1	101.0	108.6
Vinylester II (B)	105.5	102.1	103.7	111.4
Isopolyester I (C)	89.8	87.9	87.9	88.5
Isopolyester II (D)	94.7	88.2	87.9	97.9
Epoxy Amide (F)	144.2	140.4	137.9	145.0

4.4. Tests Performed

Any accelerated test method is based on a set of measurements made periodically during the duration of the test to note changes in properties of the material. A set of tests was performed for each of the three temperatures listed above. Three sets (3) of each type of the exposed specimens were removed each month for the 3-month period and tested for:

- Flexural strength and modulus of elasticity following ASTM D 790 [23]. The test specimens were supported at two points distanced 2.5 in. or 63.5 mm (support span) and loaded in a conventional "three point loading" configuration. Actual width and thickness dimensions were measured before proceeding with the test. Elastic moduli of the specimens were obtained by flexing the specimen at 73°F (23°C).
- Elastic storage moduli and glass transition temperatures were obtained by DMA (ASTM D 5023 [19]).

Flexural strength and stiffness data for 95ºF (35ºC) at 0 days (control), 28 days, and 12 months were available in the previous NFESC test program [1, 2]. They were made part of the results obtained here. For these composites, while decreases in tensile strength are mainly affected by fiber degradation, decreases in flexural strength are more affected by matrix and interface degradation. Previous testing showed that salt fog exposure of these composites would affect their flexural strength to a greater degree than tensile strength [1, 2], so the current testing was focused on flexural strength losses.

5. DEGRADATION MECHANISMS

The mechanism governing water attack on bulk glass is a combination of leaching and etching. Silicon hydroxide (SiOH) is formed as a by-product at the interface between the glass and the water. This gel layer is less dense than the original glass structure and will transport water and alkalis more readily, thus accelerating the degradation process. The addition of alumina to the glass will increase the resistance of the glass to water attack, but will actually decrease the resistance of the glass to alkalies. E-glass contains alumina and, therefore, this alkali effect should be evident. However, since the water attack eventually evolves into an alkali

attack, the addition of alumina to the glass could possibly be expected to not influence the long term overall degradation resistance of glass.

It has been shown that in the case of E-glass fibers in vinylester, the glass fibers were the critical component [15] and that the maximum moisture content of the composite was insensitive to the temperature of the environment but highly sensitive to the moisture content of the environment. Other research work indicated that the temperature of the bath would not affect the tensile strength, but the moisture content would.

Moisture has been shown to act as a plasticizer in cured thermosets, generally resulting in a reduced stiffness modulus and glass transition temperature [24]. Water acts as a plasticizer by causing physical swelling of the polymer, which can lead to increased internal stresses and micro cracking in the material [25, 26]. Plasticization disrupts Van-der-Walls bonds in the polymer chains [27, 28].

Effects of moisture sorption are potentially reversible, but may also lead to irreversible permanent effects, e.g. when hydrolysis of the molecular bonds occurs [24]. A distinction between water absorption and hydrolysis needs to be made, since they are separate phenomena [29]. Water absorption refers to the reversible physical uptake of water by the material, whereas hydrolysis is the irreversible chemical degradation of the polymer by absorbed moisture. Water absorption into a hydrolysis-sensitive polymer leads to hydrolysis.

The rate of water diffusion into the polymer is related to the polymer structure and temperature [29, 30]. The rate is lowered by the presence of nonpolar functional groups (i.e. hydrophobic groups), by branching of the polymer (steric hindrance), and by cross-linking in the polymer. The cross-linkages reduce the voids in the polymer where water may penetrate and react [30].

In the presence of electrolytes in the water, such as sodium and chloride ions from salt, diffusion is generally decreased, unless the electrolyte reacts with the polymer molecule [29]. Studies comparing epoxy, polyester, and vinyl ester GFRPs have indicated that distilled water aging over 18 months differs significantly from sea water aging in terms of weight gain (water absorption) of polyesters [31]. The use of distilled water seems to have an accelerating effect on water absorption. The vinyl ester and epoxy showed similar increases after one to three months at 50ºC in distilled water [31]. Differentiations between plasticization or alkali attack and chloride attack are not clear; that is, deterioration in the presence of chloride ions may not be attributable to chloride when water absorption is occurring or when alkali solutions are present [32].

In general, vinyl esters are the most resistant to water absorption in comparison to epoxies and polyesters [25, 32]. A study of GFRPs in deionized water and seawater at elevated temperatures revealed that epoxy and vinyl ester shear properties losses were largely recoverable after drying, whereas permanent damage occurred in the polyester composites after 18-month exposures [31]. All polyesters are hydrolyzable, but aromatic polyesters are more resistant than aliphatic polyesters [29].

The most common type of epoxy is a bisphenol-A epoxy. Its resin structure (uncured) is given in Figure 2. The end groups are called “oxirane” groups. These groups react with a “hardener”, typically an amine, to cure and cross-link the epoxy.

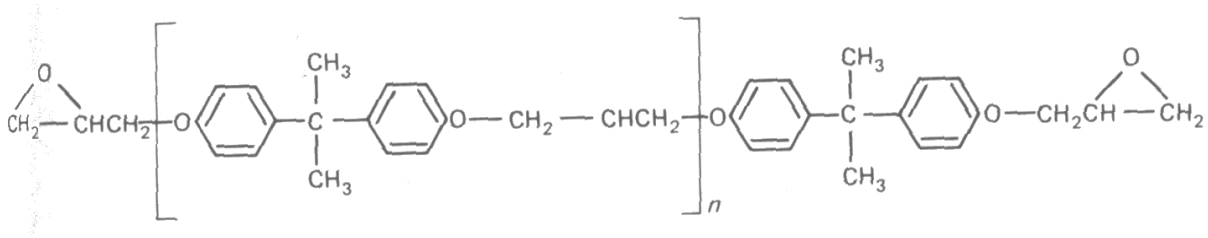

Figure 2. Bisphenol-A epoxy resin structure.

Although epoxies are known for their toughness and chemical resistance, the deleterious effects of hot and humid environments on epoxy polymers have been documented for decades and are well known [33]. As early as 1973, epoxy-graphite composites were examined for water absorption effects [34]. In this study, significant creep at room temperature, in addition to diminished rigidity, was observed.

Epoxies that are room-temperature cured are more likely to be under-cured than are epoxies cured at elevated temperatures [30]. Under-cured epoxies have reactive oxirane groups. This manifests itself in a "post-cure" when the under-cured epoxy is subsequently exposed to heat during service exposure. Post-curing causes an increase in cross-linking and thus an increase in strength of the molecular structure. A cross-linked amine-cured epoxy is represented in Figure 3.

Post-curing and plasticization can be considered as competing phenomena within the polymer during exposure to moist, hot conditions. In hydrolysis of an epoxy polymer, the oxirane epoxy groups react with water and are consumed [26]. The more under-cured the polymer, the higher the degree of plasticization [35].

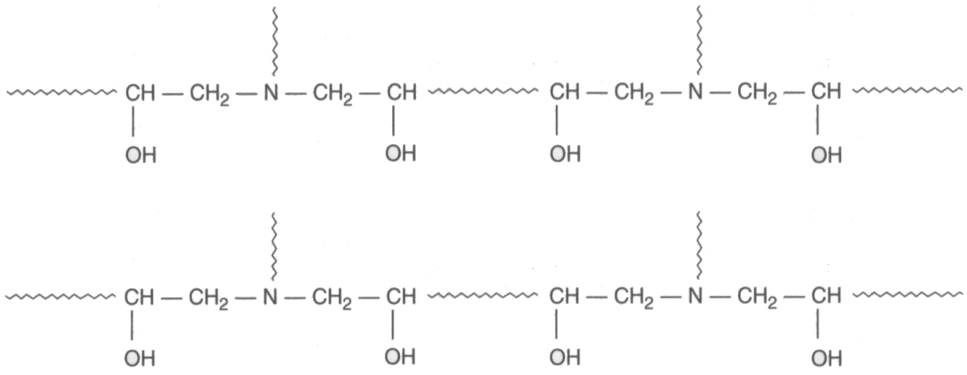

Figure 3. Cross-linked amine-cured epoxy.

Vinyl ester are now commonly used for GFRP and CFRP composites because they bond well to glass fibers and other fiber reinforcements, they process easily, and they resist a wide range of chemicals throughout the pH range [29]. Uncured vinyl ester resins can be considered as a type of acrylic polymer [36]. Cured vinyl esters, however, are thermosets. They are typically produced by reacting epoxy resins with methacrylic acids dissolved in styrene monomer. Their performance tends to fall between that of epoxy and that of unsaturated polyester. An example of a vinylester resin (uncured) is given in Figure 4.

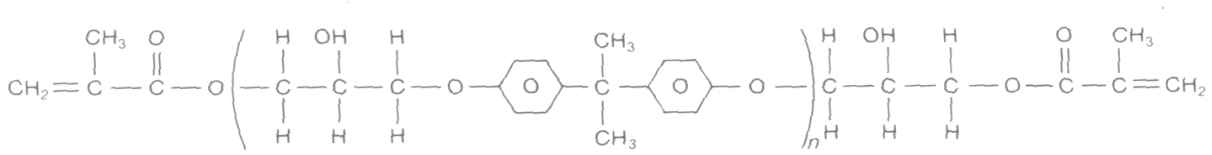

Figure 4. Uncured vinylester resin.

Compared to unsaturated polyester resins, vinyl esters have better chemical resistance. Nearby functional groups shield the ester linkages (weak in comparison to carbon-carbon bonds) from acid and base-induced hydrolysis [36]. When ester groups are hydrolyzed, usually in basic solutions, the process is often referred to as "saponification" because the reaction is analogous to the process used to convert fats to soaps. In the presence of a base such as sodium hydroxide, the carboxylic acid becomes a salt.

R-COOR'	+	OH^-	⟶	$R\text{-}COO^-$	+	R'OH
Ester Group		Hydroxide ion		Carboxylic ion		Alcohol

Glass fibers are relatively impervious to water, but are deteriorated by alkali solutions and chloride ions [25]. The corrosion mechanism of glass fibers by alkali solutions is given below [37, 38].

$$\text{-Si-O-Si-} + OH^- \longrightarrow \text{-Si-OH (solid)} + \text{-Si-O- (solution)}$$

This mechanism is known as hydroxylation and dissolution, where both a solid and a liquid by-product are formed. Hydroxylation occurs at pH values above 10 and is rapid initially, then slows as the solid by-product forms over the surface of the glass [15]. In concrete, a notching of the glass fibers occurs caused by the growth of calcium hydroxide crystals. This reduces the cross-sectional area of fiber available to resist tensile forces [15]. Aramid fibers are less susceptible to alkali environments than glass fibers [32]. Like carbon fibers, they are insensitive to chloride ions. Their susceptibility to water absorption and swelling, however, precludes their use in marine environments [25].

6. ANALYSIS OF RESULTS

6.1. Flexural tests

The flexural strength and modulus of elasticity were measured at the end of the 1-, 2-, and 3-month testing durations (details of all results are included in Appendices A through D). The plots of flexural strength and elastic modulus are shown in Appendix C. The values were then averaged for each composite, testing time, and temperature. A summary of results is shown in Tables 2 and 3. It was observed that the shift factors were not constant for different stress levels, therefore the stress-modified (t, T) parameter method was used.

Table 2a. Summary of Experimental Results for Flexural Strength, ksi (MPa).

Material	Control	T = 95ºF				T = 120ºF			T = 160ºF		
		1 mo†	2 mo	3 mo	12 mo†	1 mo	2 mo	3 mo	1 mo	2 mo	3 mo
Vinylester I	78.63	81.78	79.75	75.81	67.58	71.14	77.78	66.52	71.47	58.46	60.74
	(542.3)	(564.0)	(550.0)	(522.8)	(466.0)	(490.6)	(536.4)	(458.7)	(492.9)	(403.1)	(418.9)
Vinylester II	74.72	72.02	69.38	64.71	56.62	73.45	66.25	59.88	60.36	55.81	48.21
	(515.3)	(496.6)	(478.4)	(446.2)	(390.5)	(506.5)	(456.9)	(412.9)	(416.2)	(384.9)	(332.5)
Polyester I	85.54	75.46	72.64	83.17	57.46	82.98	66.83	63.75	63.84	55.85	52.51
	(589.93)	(520.4)	(500.9)	(573.5)	(396.2)	(572.2)	(460.9)	(439.6)	(440.2)	(385.1)	(362.1)
Polyester II	80.65	70.08	70.78	73.77	60.86	81.45	68.44	54.18	60.84	56.61	52.21
	(556.2)	(483.3)	(488.1)	(508.7)	(419.7)	(561.7)	(472.0)	(373.6)	(419.6)	(390.4)	(360.0)
Phenolic I	47.29	48.27	17.86	18.66	38.58	19.51	23.59	25.79	25.16	13.52	19.76
	(326.1)	(332.9)	(123.2)	(128.7)	(266.0)	(134.5)	(162.7)	(177.8)	(173.5)	(93.2)	(136.3)
Epoxy	94.52	72.07	67.4	67.3	62.36	69.63	61.76	60.69	53.47	45.86	49.41
	(651.9)	(497.0)	(464.8)	(464.1)	(430.0)	(480.2)	(425.9)	(418.5)	(368.7)	(316.3)	(340.7)

† These data were available from a previous NFESC project [1]

Table 2b. Summary of Experimental Results for Flexural Strength, % of control.

Material	Control	T = 95ºF				T = 120ºF			T = 160ºF		
		1 mo†	2 mo	3 mo	12 mo†	1 mo	2 mo	3 mo	1 mo	2 mo	3 mo
Vinylester I	100.0	104.0	101.4	96.4	85.9	90.5	98.9	84.6	90.9	74.3	77.2
Vinylester II	100.0	96.4	92.9	86.6	75.8	98.3	88.7	80.1	80.8	74.7	64.5
Polyester I	100.0	88.2	84.9	97.2	67.2	97.0	78.1	74.5	74.6	65.3	61.4
Polyester II	100.0	86.9	87.8	91.5	75.5	101.0	84.9	67.2	75.4	70.2	64.7
Phenolic I	100.0	102.1	37.8	39.5	81.6	41.3	49.9	54.5	53.2	28.6	41.8
Epoxy	100.0	76.2	71.3	71.2	66.0	73.7	65.3	64.2	56.6	48.5	52.3

Table 3a. Summary of Experimental Results for Stiffness, ksi (MPa).

Material	Control	T = 95ºF				T = 120ºF			T = 160ºF		
		1 mo†	2 mo	3 mo	12 mo†	1 mo	2 mo	3 mo	1 mo	2 mo	3 mo
Vinylester I	2678	2757	2568	2453	2446	2414	2387	2269	2286	1982	2168
	(18469)	(19012)	(17709)	(16916)	(16868)	(16647)	(16461)	(15647)	(15764)	(13668)	(14951)
Vinylester II	2425	2383	2206	2015	2187	2246	2171	2111	2057	2052	1952
	(16724)	(16433)	(15213)	(13895)	(15082)	(15488)	(14971)	(14557)	(14185)	(14151)	(13461)
Polyester I	2357	2168	2180	2276	1907	2148	2097	2069	2256	1940	1782
	(16255)	(14951)	(15033)	(15695)	(13151)	(14813)	(14461)	(14268)	(15557)	(13378)	(12289)
Polyester II	2253	2151	2117	2003	2147	2240	1934	1824	1849	1904	1870
	(15538)	(14833)	(14599)	(13813)	(14806)	(15447)	(13337)	(12578)	(12751)	(13130)	(12896)
Phenolic I	1995	2238	1105	1192	1879	1078	1596	1545	1498	1221	1463
	(13759)	(15433)	(7620)	(8220)	(12958)	(7434)	(11006)	(10654)	(10330)	(8420)	(10089)
Epoxy	2861	3024	2423	2449	2850	2408	2563	2523	2391	2324	2465
	(19731)	(20854)	(16709)	(16888)	(19654)	(16606)	(17674)	(17399)	(16488)	(16026)	(16999)

† These data were available from a previous NFESC project [1]

Table 3b. Summary of experimental results for stiffness, % of control.

Material	Control	T = 95ºF				T = 120ºF			T = 160ºF		
		1 mo†	2 mo	3 mo	12 mo†	1 mo	2 mo	3 mo	1 mo	2 mo	3 mo
Vinylester I	100.0	102.9	95.9	91.6	91.3	90.1	89.1	84.7	85.4	74.0	81.0
Vinylester II	100.0	98.3	91.0	83.1	90.2	92.6	89.5	87.1	84.8	84.6	80.5
Polyester I	100.0	92.0	92.5	96.6	80.9	91.1	89.0	87.8	95.7	82.3	75.6
Polyester II	100.0	95.5	94.0	88.9	95.3	99.4	85.8	81.0	82.1	84.5	83.0
Phenolic I	100.0	112.2	55.4	59.7	94.2	54.0	80.0	77.4	75.1	61.2	73.3
Epoxy	100.0	105.7	84.7	85.6	99.6	84.2	89.6	88.2	83.6	81.2	86.2

In some cases, flexural strength and stiffness initially increased despite longer exposure to the aging agent. This increase is probably due to an increase in the crosslink density. In the case of epoxy, samples are not fully cured at room temperature and additional crosslinking will take place at higher temperatures. Immersion in liquid media causes plasticization of the resin with a simultaneous reduction in T_g of the polymer.

These values of maximum stress and stiffness were plotted in a logarithmic chart and then shifted onto the 95ºF (35ºC) curves for each material. These superimposed curves are known as the master curve. It was found that the shifting factors followed a straight line behavior, which is a necessary condition for the TTS to be valid. Later, the master curve thus obtained was moved back to 70ºF (21ºC). This is the service temperature assumed for the specimens. The resulting master curves obtained are shown in Appendixes A and B. The master curves at 70ºF (21ºC) span a longer period of time, herein called maximum predictable time (MPT), but not enough to predict the degradation for a service-time length. No data fitting for extrapolation beyond the MPT was attempted due to the unknown nature of future behavior. Table 4 shows the maximum predictable time and the degradation experienced by each material.

Table 4. Predictable times and remaining flexural strength and stiffness.

Material	Flexural Strength (ksi)	Maximum predictable time (MPT) for strength	Remaining strength at MPT (%)	Stiffness (ksi)	Maximum predictable time (MPT) for stiffness	Remaining stiffness at MPT (%)
Vinylester I	78.6	4.7 years	65.2	2678	4.2 years	66.4
Vinylester II	74.7	1.4 years	64.1	2425	2 years	80.4
Polyester I	85.5	2.5 years	61.4	2357	4.2 years	75.4
Polyester II	80.7	1.6 years	64.3	2254	0.5 years	80.7
Phenolics	47.3	1.6 years	21.1	1995	dismissed†	dismissed†
Epoxy	94.5	4.7 years	40.2	2861	0.4 years	80.1

† Behavior was too erratic to be considered.

6.2. Dynamic Mechanic Analysis

Composite specimens exposed in the salt-fog chamber for 3 months at 95°F (35°C), 3 months at 120°F (49°C), and 2 months at 160°F (71°C) were tested and compared to control specimens for each type of FRP composite. Appendix D contains averaged DMA curves of exposed versus control flexural storage and loss moduli. All specimens were allowed to dry out 1 week or longer before DMA analysis. This was done in an attempt to preclude temporary effects of the moisture exposure and to capture the permanent effects of the exposure on the materials.

Interpretation of DMA curves can be difficult due to the possibility of competing chemical processes in the materials as they are exposed. The analysis of DMA results that is presented below is based on generally observed DMA behavior of thermoset resins exposed to moisture environments.

When a thermoset plastic-fiberglass composite is exposed to a moisture environment, it is generally expected that the material resin will undergo plasticization over a period of time [35, 39]. This is evidenced in the DMA data by the lowering of both flexural storage modulus values, E', and the glass transition temperature (taken as the temperature at the peak of E", the loss modulus curve). However, even if a material shows dramatic loss of storage modulus (stiffness), it may only lose a few degrees in T_g value [35].

At higher exposure temperatures, it is increasingly possible for competing reactions to affect the material. One such phenomenon is residual cross-linking or post curing of the polymer. It is not uncommon for manufactured resins to be less than 100% cured. This is not necessarily undesirable or a "flaw" in the manufacturing process. Depending on application, a slight undercure may be desirable and increases the flexibility of the material. In the case of residual cross-linking, the T_g would be expected to increase 2 to 3 degrees, depending on the degree of cross-linking [35]. A fully cured material will typically have a higher storage modulus than an under-cured specimen of the same material [35, 40]. However, the storage modulus may still decrease in a moisture exposure. This is because the more under-cured a material, the more susceptible it is to moisture damage and the greater the degree of plasticization [35, 41]. It is possible, therefore, for the resin to be plasticized and residually cross-linked, i.e. competing reactions and resulting complications in the behavior of the storage and loss moduli.

In addition to the modulus values, the overall shape of the DMA curves gives clues to the material's degree of cure or residual cross-linking [35]. A curving E' plot at temperatures below the T_g suggests a lack of cure in the specimen. This is likewise indicated by a broader E" peak. Straight line E' plots below T_g are indicative of a more fully cured or residually cross-linked specimen. This is likewise indicated by a sharper E" peak. In thermoplastic materials such as polyethylene, the shape of the curves gives indications of the amorphous nature of the material.

A phenomenon known as "vitrification" may also occur at higher temperatures [35]. Vitrification is an early form of decomposition of the polymer where the cross-linkages break down, or the material becomes amorphous. Another phenomenon seen at higher exposure temperatures is hydrolysis decomposition of the resin structure [42]. It is a severe form of plasticization. This would be expected to have a similar effect on the DMA modulus values, but with more dramatic losses.

It has been documented in the literature that a change in the exposure temperature affects the behavior of the composite material [42]. What causes an increase in the glass transition

temperature (embrittlement) of a material at one exposure temperature may cause a softening effect of the resin at another temperature.

For the various composites tested, the following was observed:

Vinyl Ester I: These exposed vinyl ester specimens showed a drop in the glass transition temperature (Table 1) for the 95°F and 120°F exposures (106.1 and 101.0°C respectively versus 108°C for the controls). This indicates a plasticizing effect on the material at these temperatures. The storage modulus values below the T_g for all of the specimens are within the range of the controls however. Overall, this vinyl ester appears to not have been significantly affected by the exposures, in terms of its elastic storage modulus.

Vinyl Ester II: These exposed vinyl ester specimens showed a decrease in the T_g (Table 1) at 95°F and 120°F exposures, but the 160°F specimens showed an increase over that of the controls (102, 103.7 and 111.4°C versus 105.5°C respectively). This would suggest some residual cross-linking might be occurring at 160°F, while plasticization is occurring at 95°F and 120°F. The 120°F E' curve below the T_g is at the lower edge of the range of the controls. The stiffness is still reduced in the 160°F exposed specimens, as evidenced by the lower starting E' values. Plasticization may also be occurring. The "straightening" and "sharpening" of the shape of both the E' and E" curves of the 160°F exposure indicates the material has residually cured.

Polyester I: These exposed isopolyester specimens all showed a decrease in the T_g (Table 1) from that of the control specimens (87.9, 87.9, and 88.5 versus 89.8°C respectively) indicating a plasticizing effect from the exposure. Only the 160°F exposure shows a significant drop in the E' flexural modulus, however, indicating a significant loss of stiffness at that temperature exposure.

Polyester II: These exposed isopolyester specimens showed a decrease in T_g (Table 1) for the 95°F and 120°F exposures from the controls (88.2 and 87.9 versus 94.7°C respectively). The 160°F exposure showed an increase in T_g (97.9°C) indicating possible residual cross-linking. Markedly lower storage modulus values, compared to the controls, were observed for all exposed specimens indicating plasticization. The E' and E" curves of the 160°F specimens are sharper in appearance, indicating residual curing is also occurring at this exposure temperature.

Phenolic: Due to erratic test behavior and a lack of proper numbers of available specimens, this material was discarded from consideration.

Epoxy: The 120° and 160°F epoxy amide specimens showed significant loss in storage modulus compared to the controls, indicating a strong plasticizing effect. The glass transition temperature was shifted to lower temperatures (Table 1) for the 95° and 120°F exposures compared to the controls (140.4 and 137.9°C versus 144.2°C) as further evidence of this effect. However the T_g of the 160°F exposure remained about the same as the controls (145°C). Epoxies are known to be especially susceptible to the plasticizing effect.

6.3. Scanning Electron Microscopy

SEM pictures of the epoxy composite were taken after 3-month exposure at 120°F, and shown in Figure 5 and Figure 6 along with their corresponding control surfaces. This material experienced a 36% flexural strength degradation after such exposure. Prior to the examination, all samples were prepared to a half-micron final polish. They were subsequently sputter coated with gold palladium.

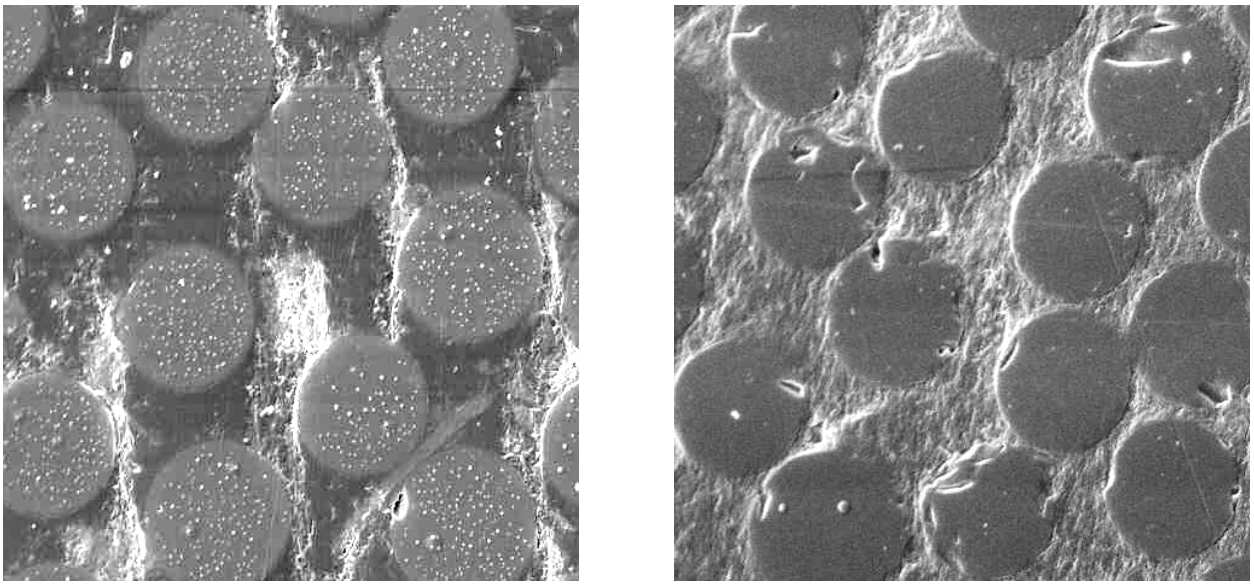

(a) (b)

Figure 5. Control (a) and exposed (b) epoxy composite SEM scans (500x).

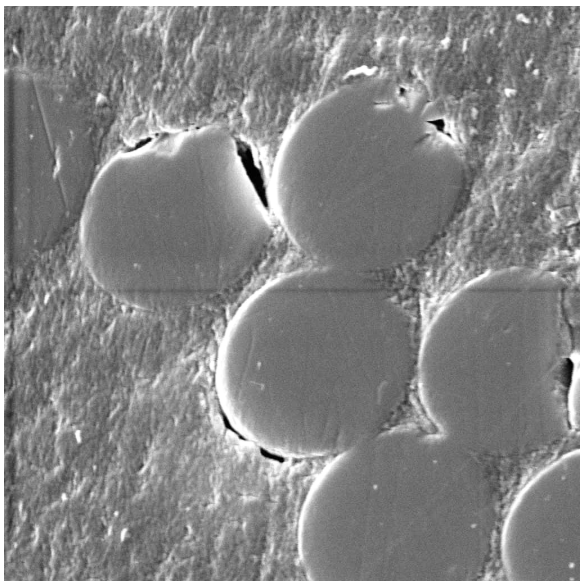

Figure 6. Exposed epoxy composite SEM scan (2000x).

The SEM pictures show significant amounts of surface fiber degradation and interface damage, as shown by the dark pits and cracks (Figure 5b). This type of damage was also reported by Grant and Bradley [43]. As previously noted, the damage mechanism is a combination of leaching and etching, probably caused by the formation of SiOH at the interface between the glass and the water.

6.4. Minimum Allowable Values

The data that were obtained under this exposure may be used to determine minimum allowable values for the flexural strength, the ultimate elongation, and the Young's modulus. For example, CALTRANS has established criteria to determine those minimum values [7]: the Young's modulus, strength and strain are estimated after exposure to 1,000 hours, 3,000 hours and 10,000 hours (41, 125, and 416 days respectively) to several aggressive environments (the minimum values are estimated as the mean of three tests minus two or three standard deviations). The accelerated technique could be used to shorten the exposure times, or to make those exposure times representative of longer actual environmental exposure conditions. ACI 440 [13] recommends that glass bars in concrete exposed to earth and weather must use an environmental exposure reduction factor of 0.7 – the current results could be used to establish similar or even more severe factors for flexural applications, depending on the structure life expectancy, bar protection, and bar diameter. Alternatively, an expected service life could be proposed, during which the remaining strength after exposure could not be less than a certain percentage of the measured short-term property. While the current results provide a preliminary insight into the expected degradation, additional testing would be needed to allow time extrapolation in the order of the structure's life expectancy.

7. CONCLUSIONS

A testing program for accelerating aging in GFRP has been conducted under salt-fog exposure. The resulting high degradation raises serious questions about the durability of composites under this simulated marine exposure. The degradation experienced by these specimens did not allow for a long-term evaluation of their behavior. However, the short-term behavior was significant enough to report and to warrant further research into the effect of salt water on composites.

From the laboratory results and the time-temperature superposition technique, more specific conclusions can be drawn:

1. In the short test time, the degradations experienced by most of the materials were significant enough to compromise their long-term flexural strength (losses of 35% or more in less than five years in all cases).
2. Salt-fog exposure seemed to affect the flexural strengths of the composites to a much larger degree than they affected the moduli, an observation previously reported in the literature [44].
3. Phenolics seems to be unfit for this type of exposure due to the significant degradation (~60%) expected in a short time (20 months). Glass reinforced phenolics had an erratic behavior making predictions unreliable. The significant variation in both exposed and unexposed specimen properties also points to difficulties and nonuniformity in the phenolics fabrication process.

4. Glass-reinforced vinylester seems to be the most convenient material for this exposure given the lesser degradation (~35%) over a five-year period. The superior performance of vinylester relative to polyester resin in typical industrial corrosive environments has been well documented [45, 21].
5. With glass-reinforced vinylester, the stiffness degradation is also the least, averaging 25% in roughly the same time.
6. The degradations experienced by the specimens were not enough to extrapolate into service-life expectancy (50-100 years) of concrete structures. Additional testing is needed for longer predictions.
7. Further research is required to determine a procedure to incorporate these results into an effective safety factor.

8. ACKNOWLEDGEMENTS

Funding for this project was provided by the Office of Naval Research under Dr. Ignacio Perez. Professor Arsenio Caceres, from the University of Puerto Rico, was on leave at NFESC under the Navy Summer Faculty Research Program sponsored by the Office of Naval Research and administered by the American Society of Engineering Education.

Dan Polly kindly assisted in the preparation of samples and operation of the SEM for the pictures shown in this report. Specimens and support provided by Dr. Tom Novinson are gratefully acknowledged.

9. REFERENCES

1. Jamond, R.M., Hoffard, T.A., Novinson, T., Malvar, L.J., *"Composites in Simulated Marine Environments*," NFESC Special Publication SP-2083-SHR, May 2000.
2. Malvar, L.J., Jamond, R.M., Hoffard T.A., Novinson T., *"GFRP Composites in Simulated Marine Environments,"* 2nd International Conference on Durability of FRP Composites for Construction, CDCC'02, Montreal, Quebec, Canada, May 2002, pp. 191-202.
3. Caceres, A., Jamond, R.M., Hoffard, T.A., Malvar, L.J., *"Accelerated Testing of Fiber Reinforced Polymer Matrix Composites – Test Plan,"* NFESC Special Publication SP-2091-SHR, August 2000.
4. Porter, M.L., Barnes, B.A., *"Accelerated Aging Degradation of Glass Fiber Composites,"* Fiber Composites in Infrastructure, Vol. II, Second International Conference on Composites in Infrastructure, Tucson, AZ, January 1998, pp. 446-459.
5. Bank, L.C., Gentry, T.R., Barkatt, A., Prian, L., Wang, F., Mangla, S. R., *"Accelerated Aging of Pultruded Glass/Vinylester Rods,"* Fiber Composites in Infrastructure, Second

International Conference on Composites in Infrastructure, Tucson, AZ, January 1998, pp. 423-437.
6. Chajes, M.J, Thomson, T.A., Farschman, C.A., *"Durability of Concrete Beams Externally Reinforced with Composite Fabrics,"* Journal of Construction and Building Materials, Vol. 9, No. 3, 1995, pp. 141-148.
7. Sheng, L., *"Summary of CALTRANS' FRP Composite Pre-Qualification Program,"* 46th International SAMPE Symposium Proceedings, Vol. 1, May 2001, pp. 923-930.
8. Sultan, M., Hawkins, G., Sheng, L-H., *"CALTRANS Program for the Evaluation of Fiber Reinforced Plastics for Seismic Retrofit and Rehabilitation of Structures,"* Proceedings, FHWA National Seismic Conference, San Diego, CA, 1995.
9. International Conference of Building Officials, Evaluation Service, *"Acceptance Criteria for Concrete and Reinforced and Unreinforced Masonry, Strengthening using Fibre-Reinforced, Composite Systems,"* AC125, International Conference of Building Officials, Whittier, CA, 1997.
10. Sonobe, Y., Fukuyama, H., Okamoto, T., Kani, N., Kimura, K., Kobayashi, K., Masuda, Y., Matsuzaki, Y., Mochizuki, S., Nagasaka, T., Shimizu, A., Tanano, H., Tanigaki, M., Teshigawara, M., *"Design Guidelines of FRP Reinforced Concrete Building Structures,"* Journal of Composites for Construction, Vol. 1, No. 3, 1997, pp. 90-113.
11. CHBDC Technical Committee 16, *"Design Provisions for Fibre Reinforced Structures in the Canadian Highway Bridge Design Code,"* Second International Conference on Advanced Composite Materials in Bridges and Structures, Montreal, Quebec, Canada, 1996, pp. 391-406.
12. Canadian Standards Association, *Canadian Highway Bridge Design Code,* Section 16: Fibre Reinforced Structures, and Commentary, Canadian Standards Association, 2001, 28 pp.
13. American Concrete Institute Committee 440, *"Guide for the Design and Construction of Concrete Reinforced with FRP Bars,"* ACI 440.1R-01, American Concrete Institute, 2001.
14. American Concrete Institute Committee 440, *"Guide for the Design and Construction of Externally Bonded FRP Systems for Strengthening Concrete Structures,"* ACI 440.2R-02, American Concrete Institute, 2002.
15. Metcalfe, A.G., Schmitz, G.Z., *"Mechanism of Stress Corrosion in E-Glass Filaments,"* Glass Technology, Vol. 13, No. 1, pp. 5-16, February 1972.
16. Proctor, B.A., *"The Long Term Behaviour of GlassFibre Reinforced Composites,"* Proceedings NATO Advanced Study Institute, Tenerife, Spain, Wright A. F. and Dupuy J. ed., NATO Science Committee, April 1984, pp. 530-550.
17. Iyer, C.V., Balachandar, M.A., Raghavan, J., *"Long-term Durability of Polymer Composites,"* 46th International SAMPE Symposium Proceedings, Vol. 1, May 2001, pp. 704-717.
18. ASTM B 117, *"Standard Practice for Operating Salt Spray (Fog) Apparatus,"* Annual Book of Standards, American Society for Testing and Materials, 1995.
19. ASTM D 4065, *"Standard Practice for Plastics: Dynamic Mechanical Properties: Determination and Report of Procedures",* Annual Book of Standards, American Society for Testing and Materials, 1995.
20. ASTM D 5023, *"Standard Test Method for Measuring the Dynamic Mechanical Properties: In Flexure (Three-Point Bending)",* Annual Book of Standards, American Society for Testing and Materials, 1995.

21. Gentry, T. R., Bank, L. C., Thompson, B. P., Russel, J. S., *"An Accelerated-Test-Based Specification for Fiber Reinforced Plastics for Structural Systems,"* Second International Conference on Durability of Fiber Reinforced Polymer (FRP) Composites for Construction (CDCC 02), Montreal, Quebec, Canada, May 2002, pp. 13-24.
22. Chin, J.W., Nguyen, T., Aouadi, K., *"Effects of Environmental Exposure on Fiber-Reinforced Plastic (FRP) Materials Used in Construction,"* Journal of Composites Technology & Research, JCTRER, Vol. 19, No. 4, 1997, pp. 205-213.
23. ASTM D 790, *"Standard Test Methods for Flexural Properties of Unreinforced and Reinforced Plastics and Electrical Insulating Materials,"* Annual Book of Standards, American Society for Testing and Materials, 1995.
24. Turi, E.A., *"Thermal Characterization of Polymeric Materials",* Academic Press, Inc., Orlando, FL, 1999.
25. Balazs, G.L., and Borosnyoi, *"Long-term Behavior of FRP",* International Workshop on Composites in Construction - A Reality, International Center for Scientific Culture of Naples University, Capri, Italy, 2001, pp. 84-91.
26. Wicks, Z.W., Jones, F.N., Pappas, S.P., *"Organic Coatings Science and Technology",* John Wiley & Sons, New York, 1999.
27. Bank, L.C., Gentry, T.R., Barkatt, A., *"Accelerated Test Methods to Determine the Long-term Behavior of FRP Composite Structures: Environmental Effects",* Journal of Reinforced Plastics and Composites, Vol. 14, No. 6, 1995, pp. 559-587.
28. Wang, P., Masmoudi, R., Benmokrane, B., *"Durability of GFRP Bars: Assessment and Improvement",* Second International Conference on Durability of Fiber Reinforced Polymer (FRP) Composites for Construction, CDCC'02, University of Sherbrooke, Montreal, Canada, 2002, pp. 153-163.
29. Dostal, C.A., ed., *"Engineering Plastics",* Engineered Materials Handbook, Vol. 2, ASM International, 1988.
30. Ferrier, E., Hamelin, P., *"Effect of Water Absorption on the Durability of Carbon FRP Reinforcement",* Second International Conference on Durability of Fibre Reinforced Polymer (FRP) Composites for Construction, CDCC'02, University of Sherbrooke, Montreal, Canada, pp. 99-112, 2002,
31. Davies, P., Mazeas, F., Casari, P., *"Sea Water Aging of Glass Reinforced Composites: Shear Behavior and Damage Modelling",* Journal of Composite Materials, Vol. 35, No. 15, 2001, pp. 1343-1372.
32. Waldron, P., Byars, E.A., and Dejke, V., *"Durability of FRP in Concrete - A State of the Art,"* International Workshop on Composites in Construction - A Reality, International Center for Scientific Culture of Naples University, Capri, Italy, 2001, pp. 92-101.
33. Davis, A., Grassie, N. (Editors), *"Developments in Polymer Degradation",* Applied Science Publishers, London, 1977.
34. McKague, E.L., Reynolds, J.D., Halkias, J.E., *"Thermomechanical Testing of Plastics for Environmental Resistance",* Journal of Testing and Evaluation, Vol. 1, No. 6, 1973, pp. 468-471.
35. Personal communications with technical representatives at TA Instruments, a manufacturer of DMA and other thermal analysis equipment, various dates, 2001.
36. Hare, C.H., *"Protective Coatings Fundamentals of Chemistry and Composition",* Technology Publishing Company / SSPC, Pittsburgh, 1994.

37. Kajorncheappunngam, S., Gupta, R.K., Gangarao, H.V.S., *"Effect of Aging Environment on Degradation of Glass-Reinforced Epoxy",* Journal of Composites for Construction, Vol. 6, No. 1, 2002, pp. 61-69.
38. Nkurunziza, G., Masmoudi, R., Benmokrane, B., *"Effect of Sustained Tensile Stress and Temperature on Residual Strength of GFRP Composite Bars",* Second International Conference on Durability of Fibre Reinforced Polymer (FRP) Composites for Construction, CDCC'02, University of Sherbrooke, Montreal, Canada, 2002, pp. 347-358.
39. Wang, J. and Ploehn, J, *"Dynamic Mechanical Analysis of the Effect of Water on Glass Bead-Epoxy Composites,"* Journal of Applied Polymer Science, Vol. 59, 1996, pp. 345-357.
40. Cordovez, M., Li, Y., Karbhari, V.M., *"Use of Dielectrometry Process and Health Monitoring of FRP Composites,"* 2nd Conference on Durability of Fiber-Reinforced Polymer (FRP) Composites for Construction, CDCC'02, May 2002, pp. 499-510.
41. Chu, W. and Karbhari, V.M., *"Characterization and Modeling of Moisture and Alkali Effects on E-Glass/Vinylester Composites,"* Second International Conference on Durability of Fiber-Reinforced Polymer (FRP) Composites for Construction, CDCC'02, Montreal, Quebec, May 2002, pp. 359-369.
42. Helbling, C.S., and Karbhari, V.M., *"Environmental Durability of E-Glass/Vinylester Composites Under the Combined Effect of Moisture, Temperature, and Stress,"* Second Conference on Durability of Fiber-Reinforced Polymer (FRP) Composites for Construction, CDCC'02, Montreal, Quebec, May 2002, pp. 247-258.
43. Grant, T.S., Bradley, W.L., *"In-Situ Observations in SEM of Degradation of Graphite/Epoxy Composite Due to Seawater Immersion",* Journal of Composite Materials, Vol. 29, No. 7, 1995, pp. 852-867.
44. Bank, L. C., Barkatt, A., Gentry, T. T., and Prian, L., *"Use of Physicochemical, Mechanical and Optical Tests in Accelerated Test Methodology for Determining the Long-Term Behavior of FRP Composites,"* Report to the Federal Highway Administration contract DTFH61-93-C-00012, 1997, 94 pp.
45. Bank, L. C., *"Properties of FRP Reinforcements for Concrete,"* Fiber-Reinforced Plastic (FRP) for Concrete Structures: Properties and Applications, (A. Nanni, ed.), Elsevier Science Publishers, Amsterdam, The Netherlands, 1993, pp. 59-86.

Appendix A: Master Curves for Flexural Strength at T = 70º F

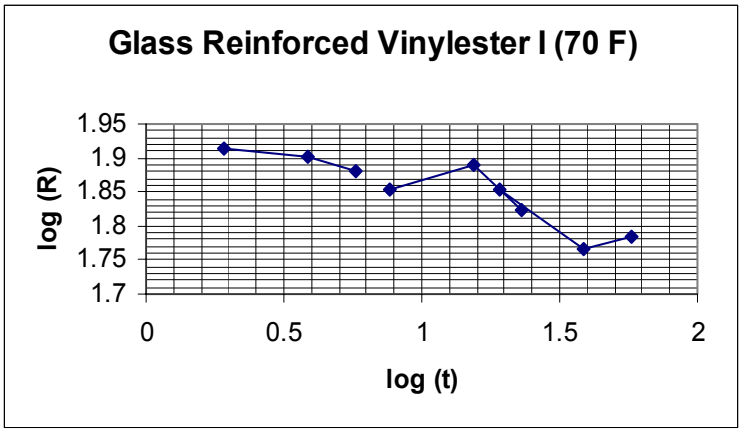

Figure A-1. Master curve for Vinylester I at 70º F.

(Note: in all graphs, flexural strength R is in ksi, and time in months)

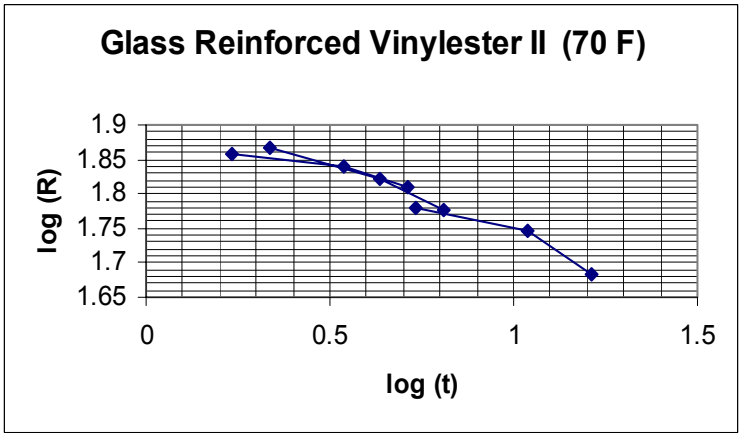

Figure A-2. Master curve for Vinylester II at 70º F.

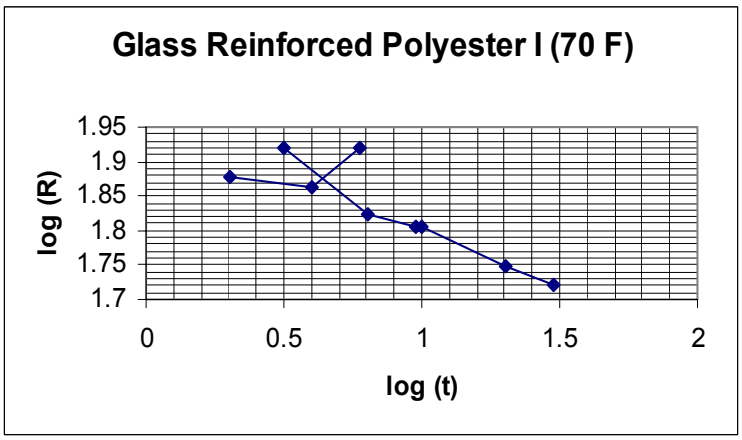

Figure A-3. Master curve for Polyester I at 70º F.

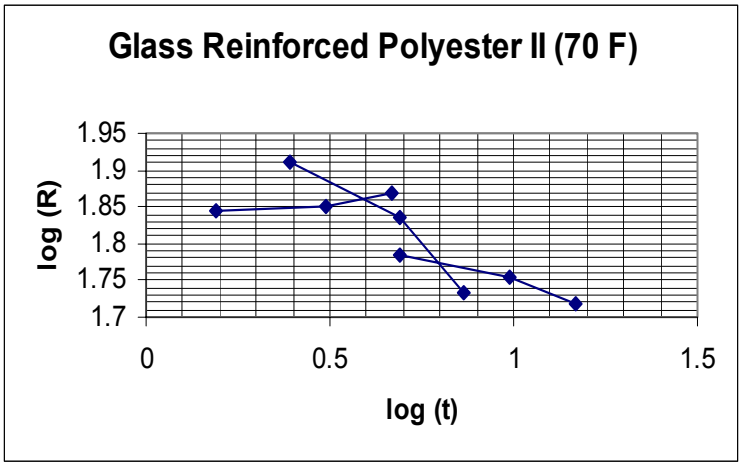

Figure A-4. Master curve for Polyester II at 70º F.

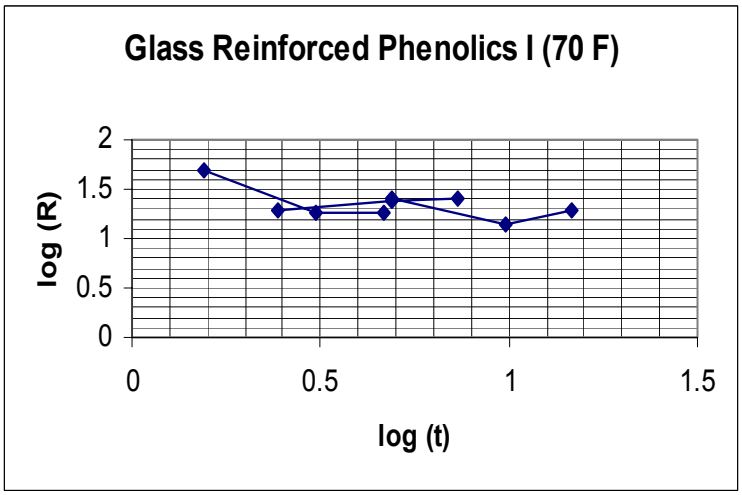

Figure A-5. Master curve for Phenolic I at 70º F.

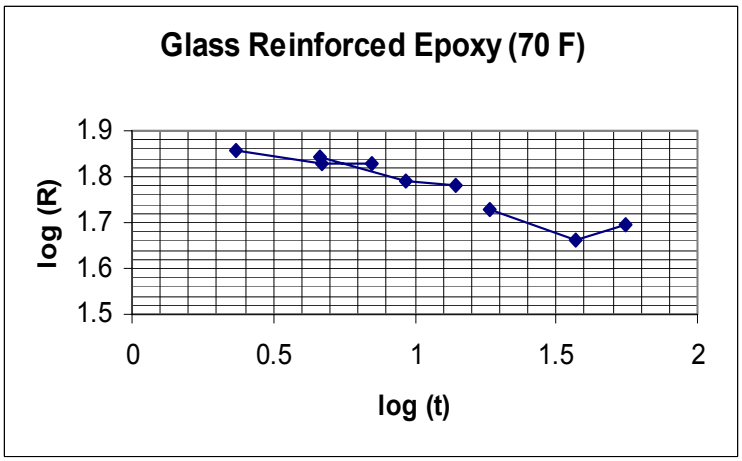

Figure A-6. Master curve for Epoxy at 70º F.

Appendix B: Master Curves for Stiffness at T = 70º F

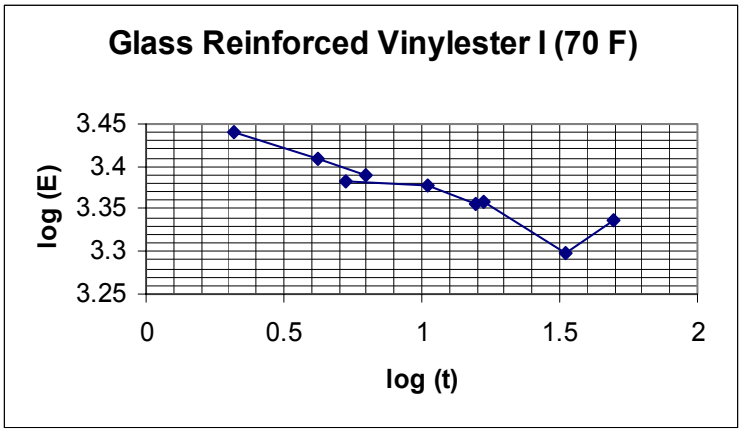

Figure B-1. Master curve (stiffness) for Vinylester I at 70º F.

(Note: in all graphs, stiffness E is in ksi, and time in months)

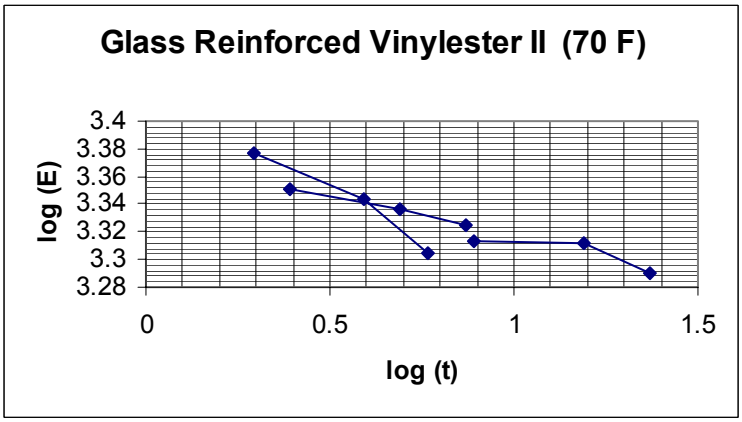

Figure B-2. Master curve (stiffness) for Vinylester II at 70º F.

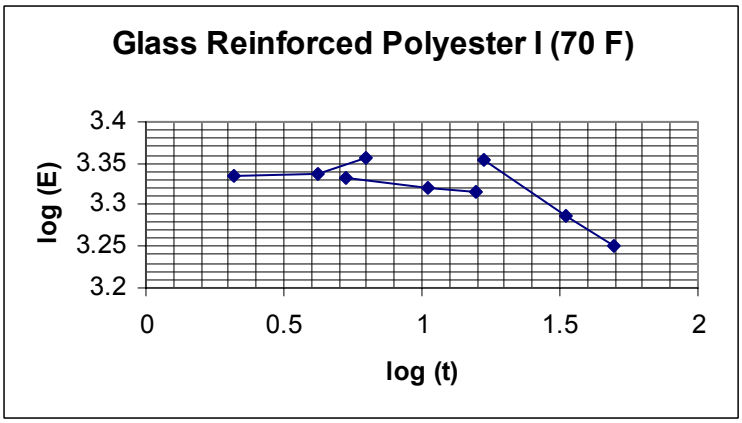

Figure B-3. Master curve (stiffness) for Polyester I at 70º F.

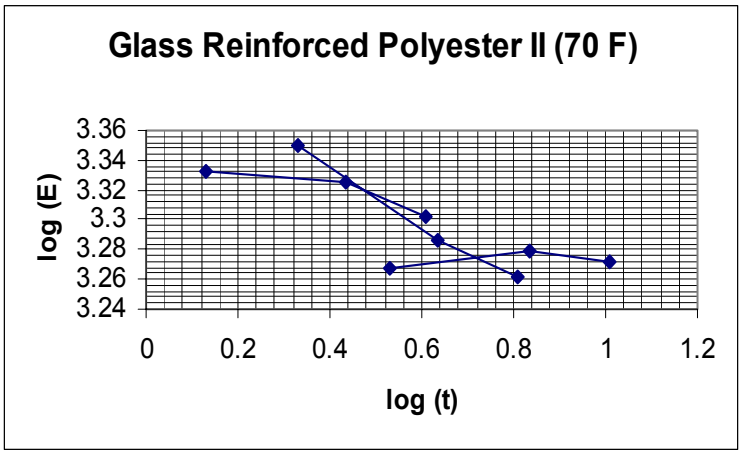

Figure B-4. Master curve (stiffness) for Polyester II at 70º F.

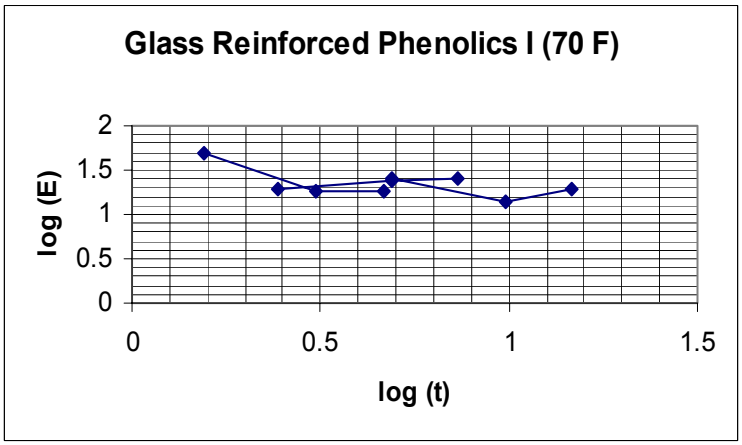

Figure B-5. Master curve (stiffness) for Phenolic I at 70º F.

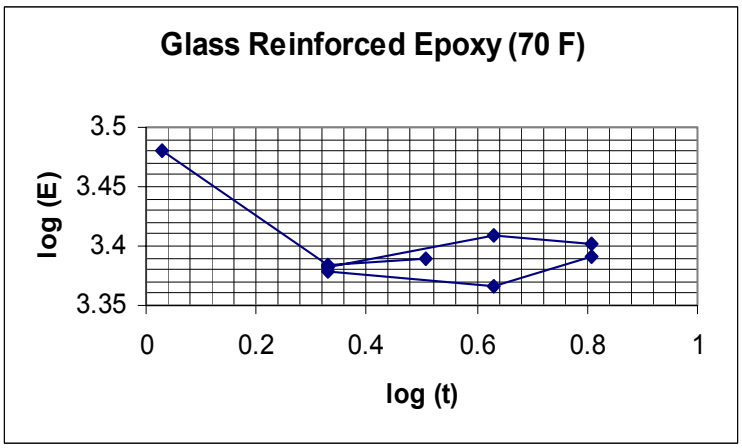

Figure B-6. Master curve (stiffness) for Epoxy at 70º F.

Appendix C: Flexural Test Curves

All stresses, elastic and inelastic, in the following charts were computed using the elastic formula for flexure: $\sigma_{max} = 3PL/2bh^2$. Curves for 1 month and 12 months at 95º F can be found in Reference [1].

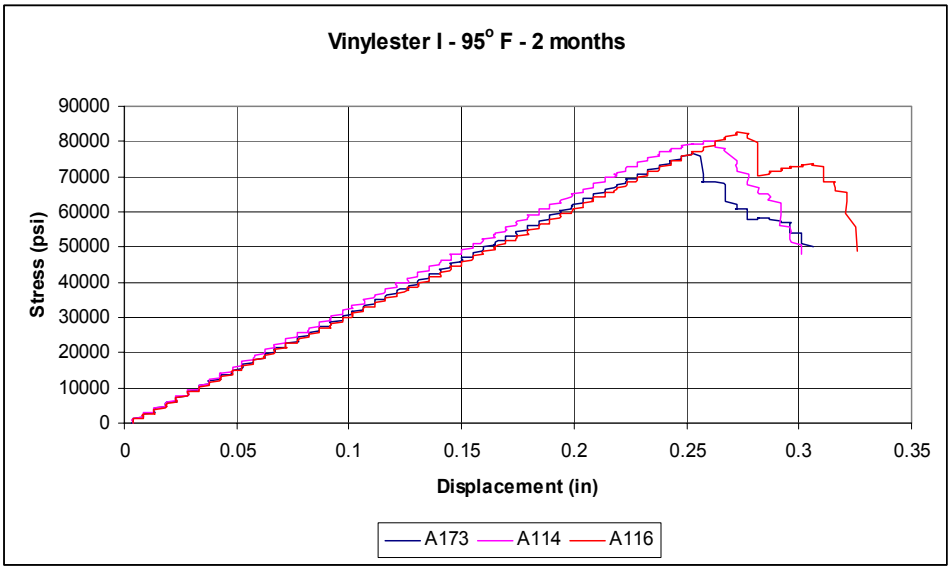

Figure C-1. Flexural test curves for Vinylester I after 2 months at 95ºF.

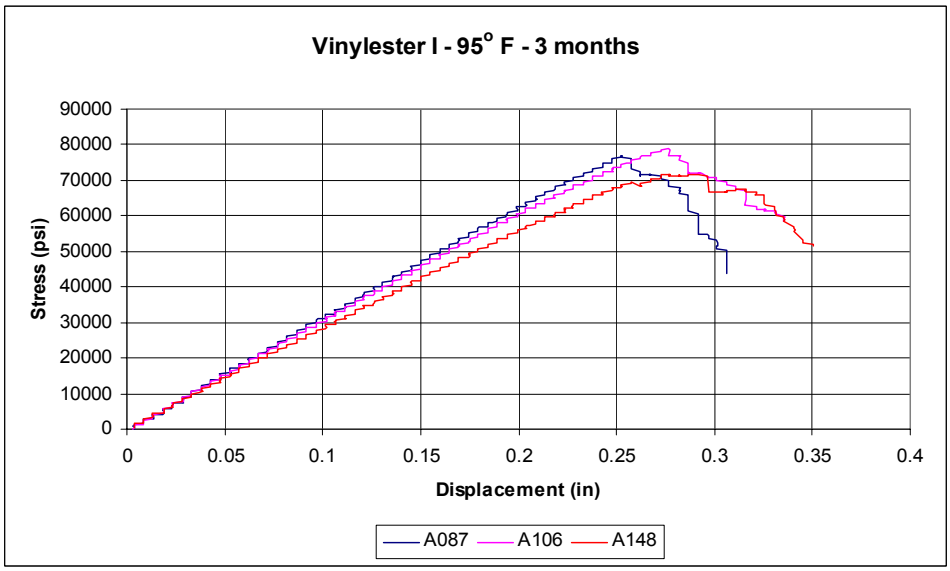

Figure C-2. Flexural test curves for Vinylester I after 3 months at 95ºF.

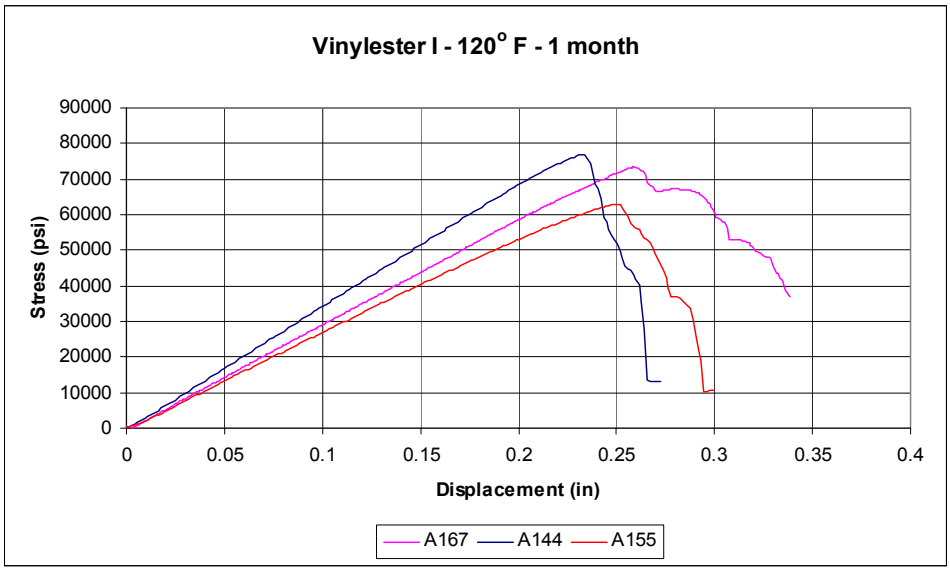

Figure C-3. Flexural test curves for Vinylester I after 1 month at 120ºF.

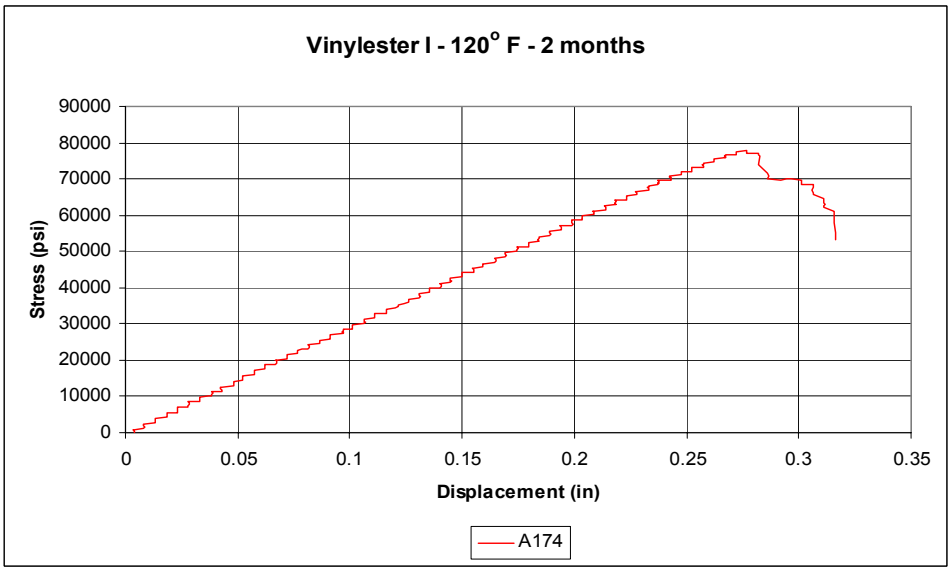

Figure C-4. Flexural test curves for Vinylester I after 2 months at 120ºF.

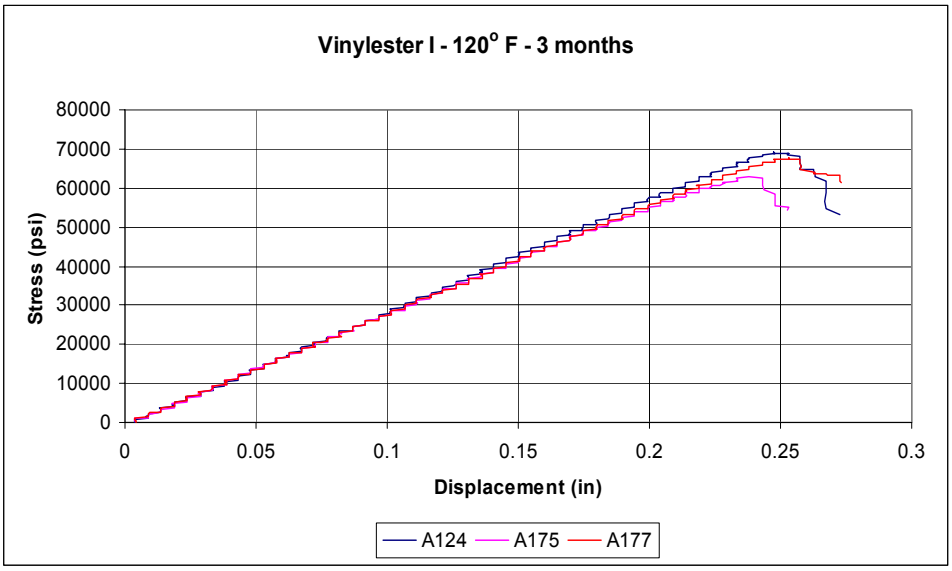

Figure C-5. Flexural test curves for Vinylester I after 3 months at 120ºF.

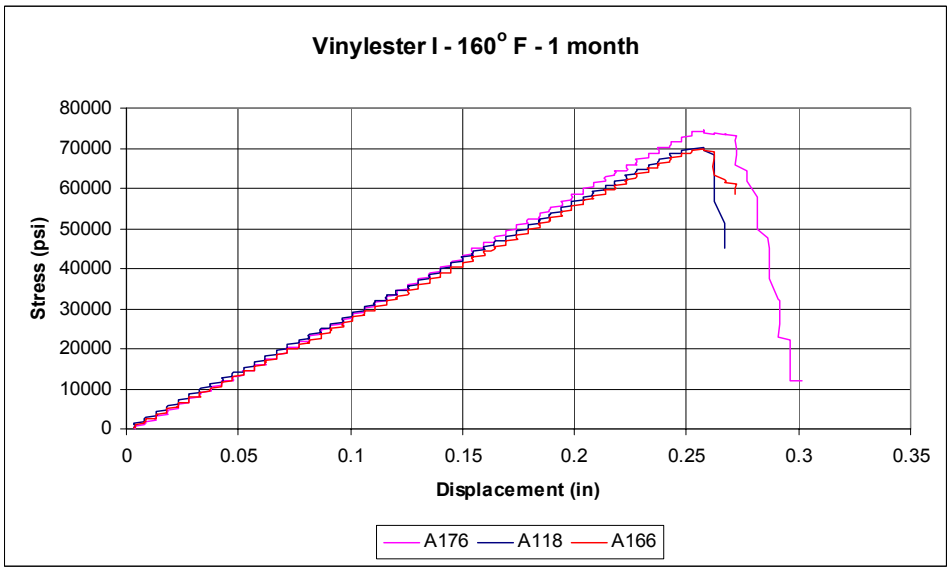

Figure C-6. Flexural test curves for Vinylester I after 1 month at 160ºF.

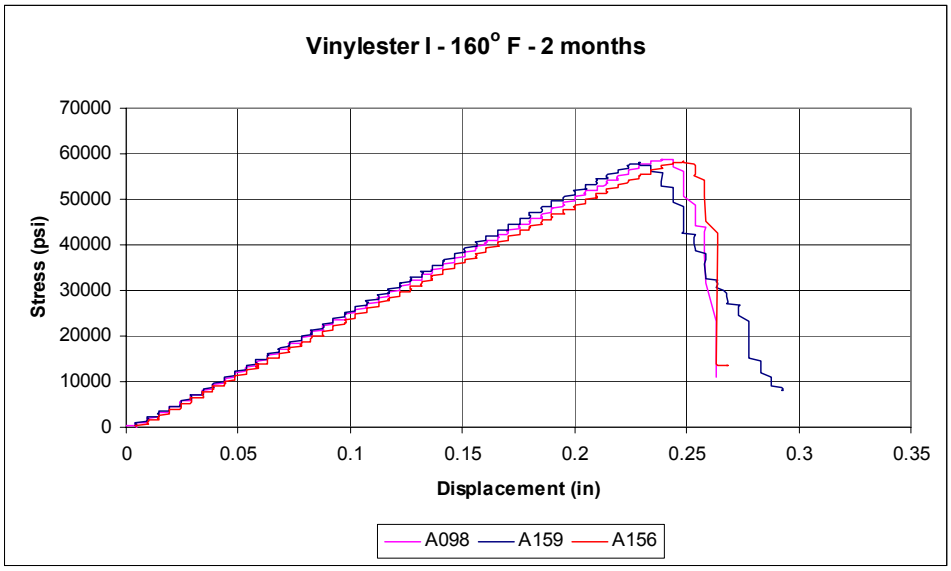

Figure C-7. Flexural test curves for Vinylester I after 2 months at 160ºF.

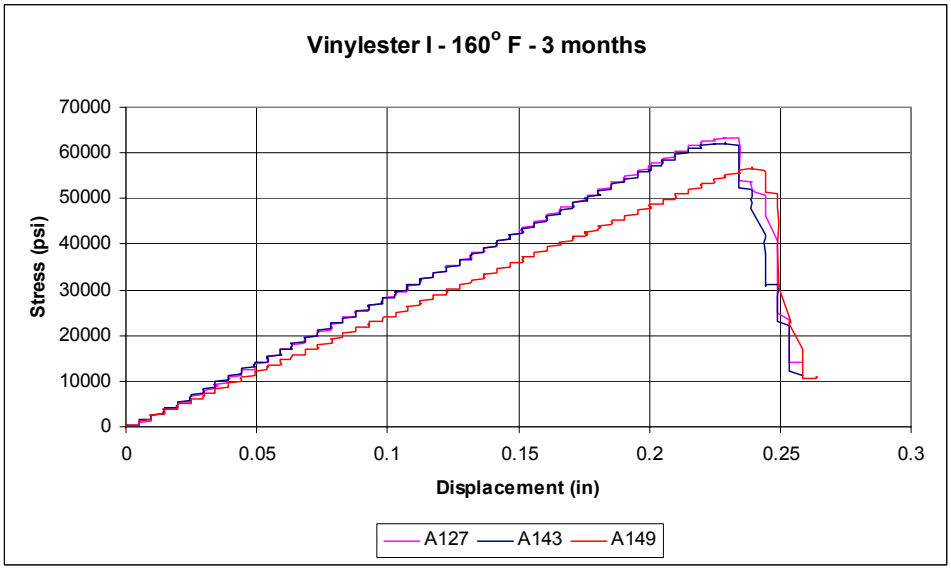

Figure C-8. Flexural test curves for Vinylester I after 3 months at 160ºF.

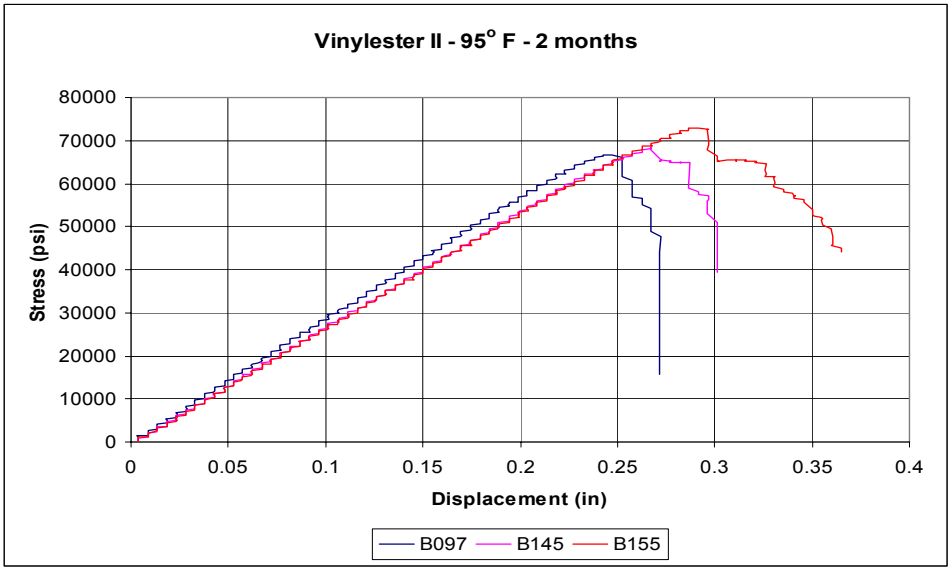

Figure C-9. Flexural test curves for Vinylester II after 2 months at 95ºF.

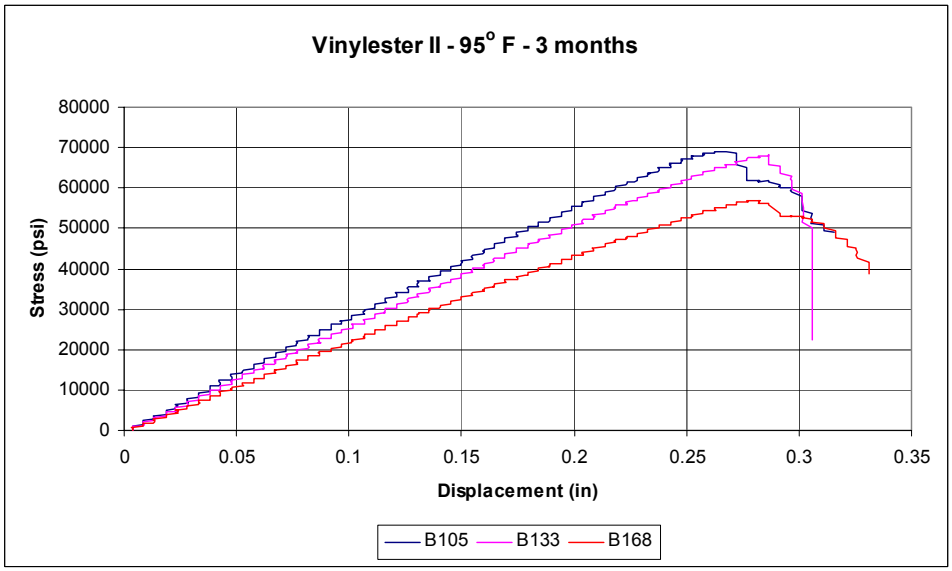

Figure C-10. Flexural test curves for Vinylester II after 3 months at 95ºF.

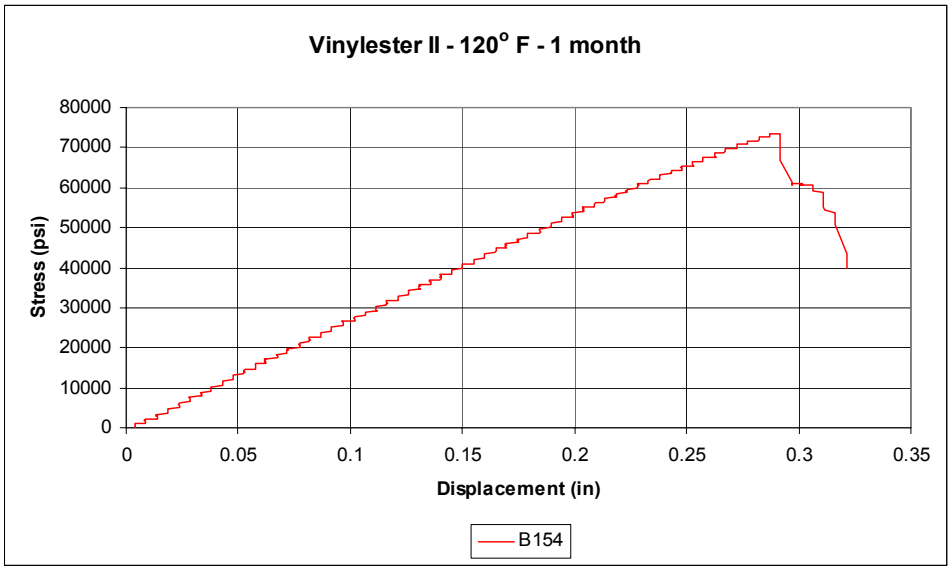

Figure C-11. Flexural test curves for Vinylester II after 1 month at 120ºF.

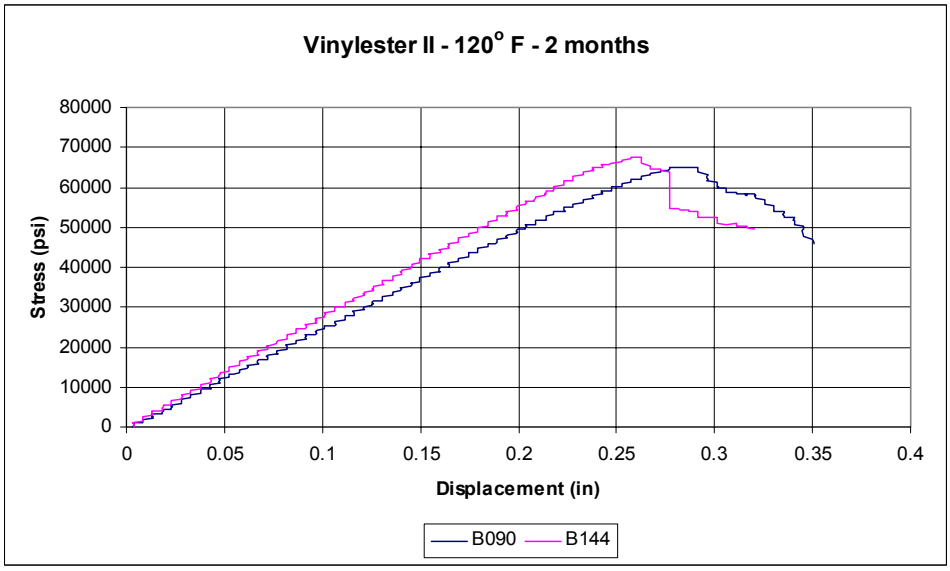

Figure C-12. Flexural test curves for Vinylester II after 2 months at 120ºF.

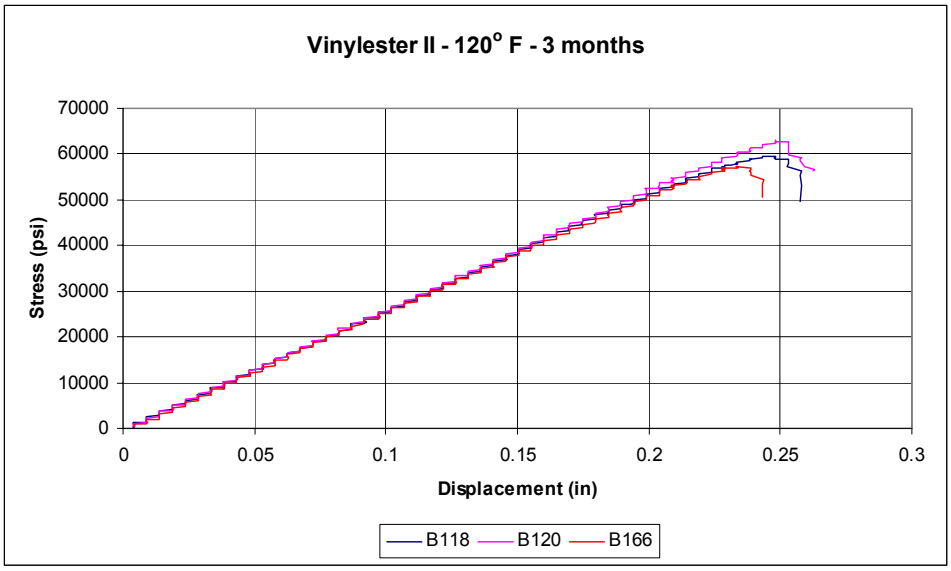

Figure C-13. Flexural test curves for Vinylester II after 3 months at 120ºF.

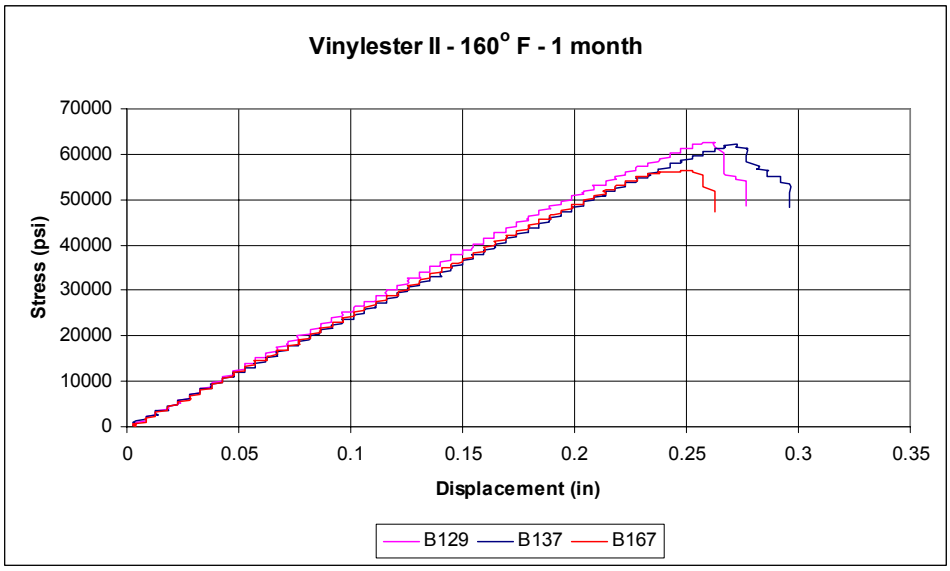

Figure C-14. Flexural test curves for Vinylester II after 1 months at 160ºF.

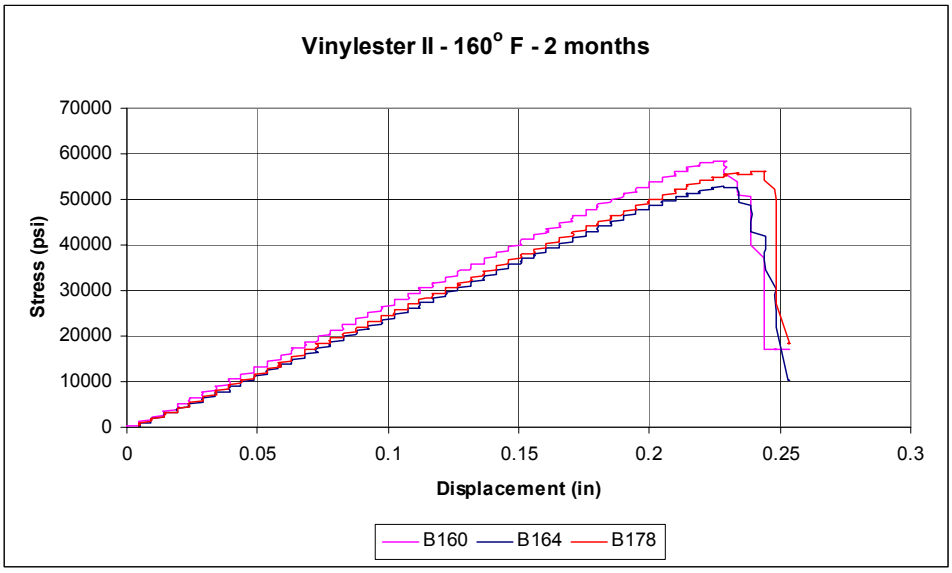

Figure C-15. Flexural test curves for Vinylester II after 2 months at 160ºF.

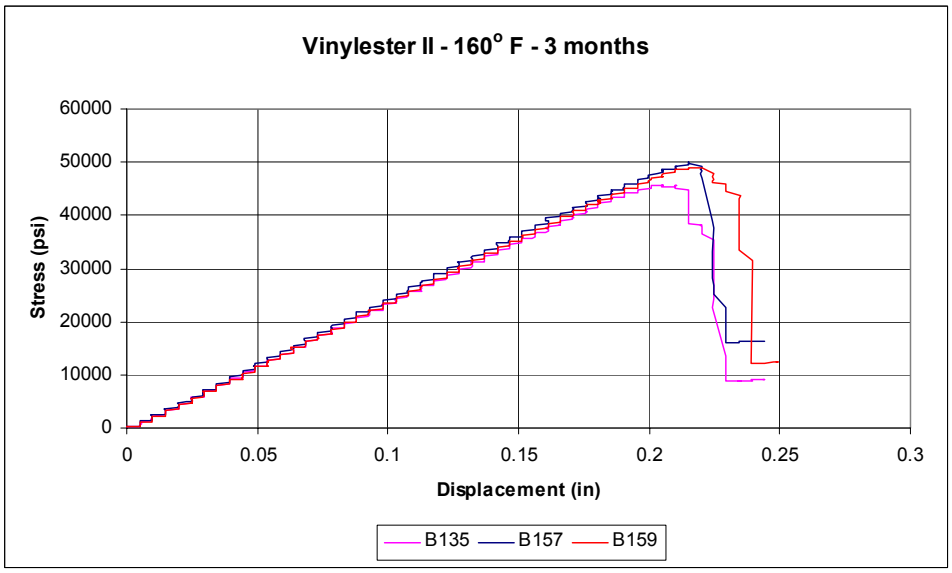

Figure C-16. Flexural test curves for Vinylester II after 3 months at 160ºF.

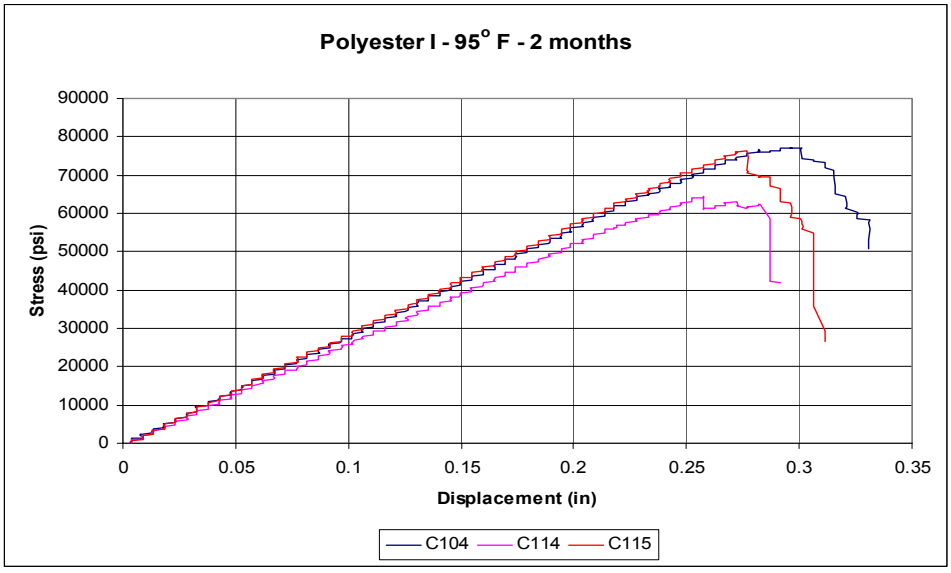

Figure C-17. Flexural test curves for Polyester I after 2 months at 95ºF.

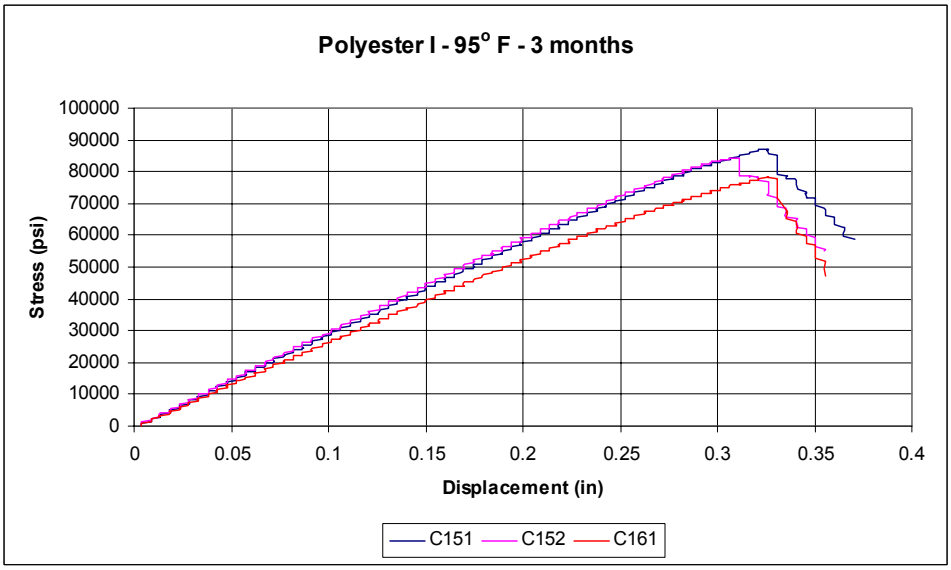

Figure C-18. Flexural test curves for Polyester I after 3 months at 95ºF.

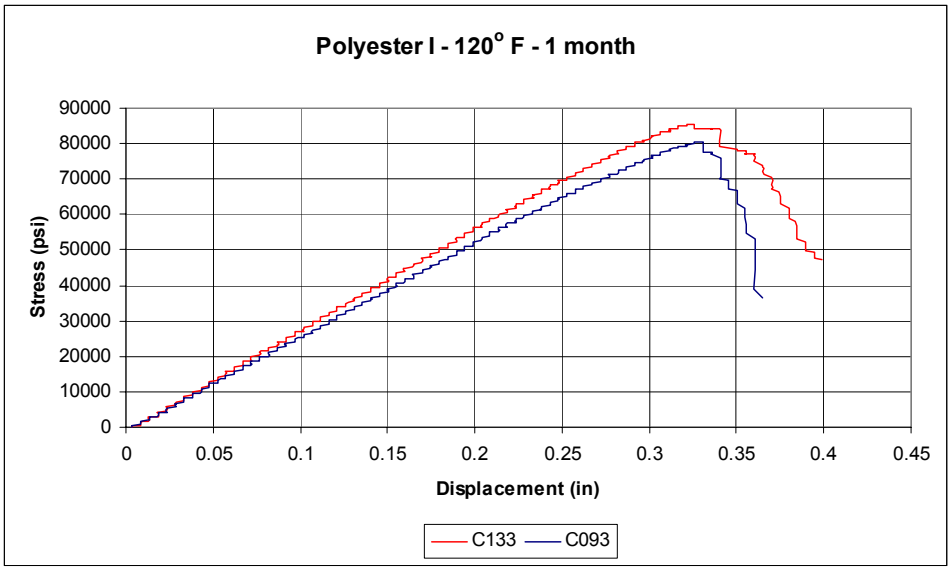

Figure C-19. Flexural test curves for Polyester I after 1 month at 120ºF.

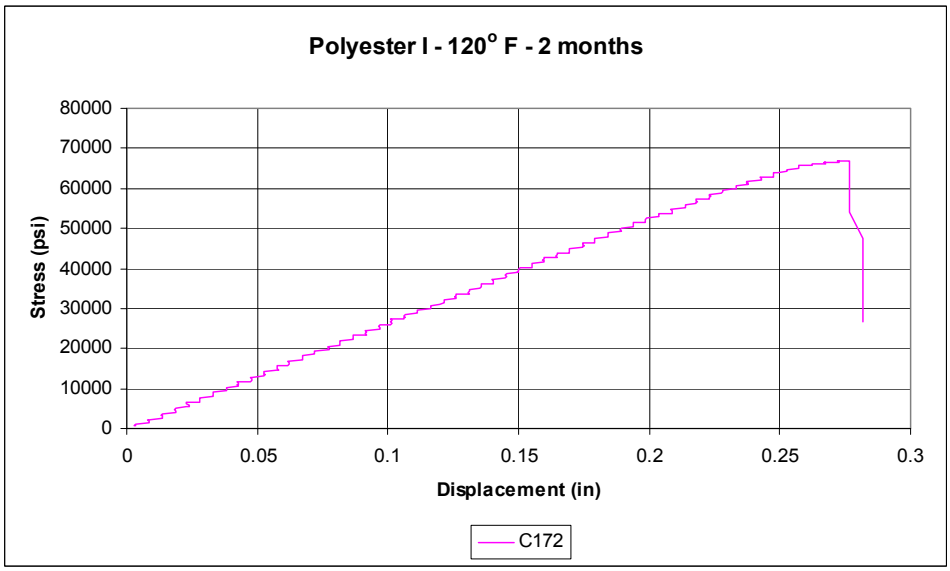

Figure C-20. Flexural test curves for Polyester I after 2 months at 120ºF.

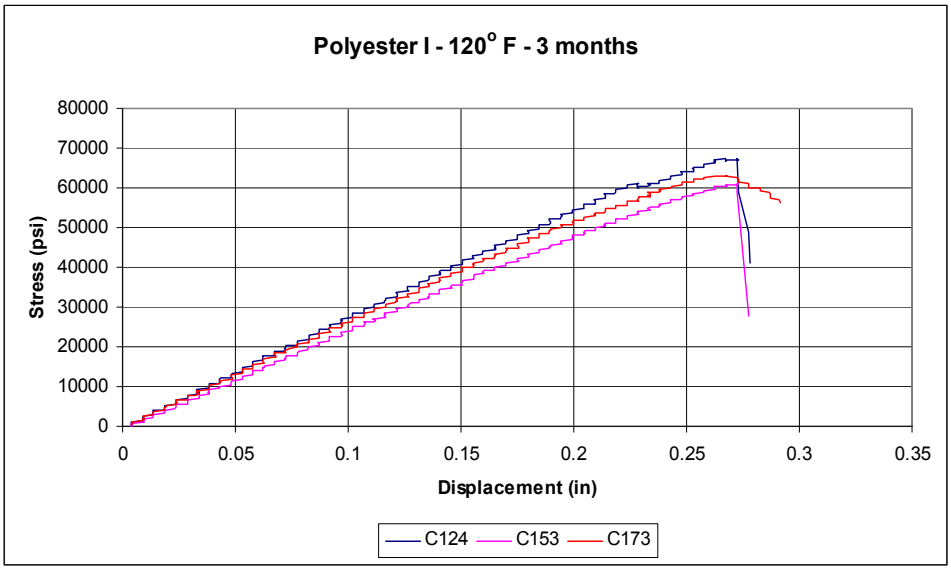

Figure C-21. Flexural test curves for Polyester I after 3 months at 120ºF.

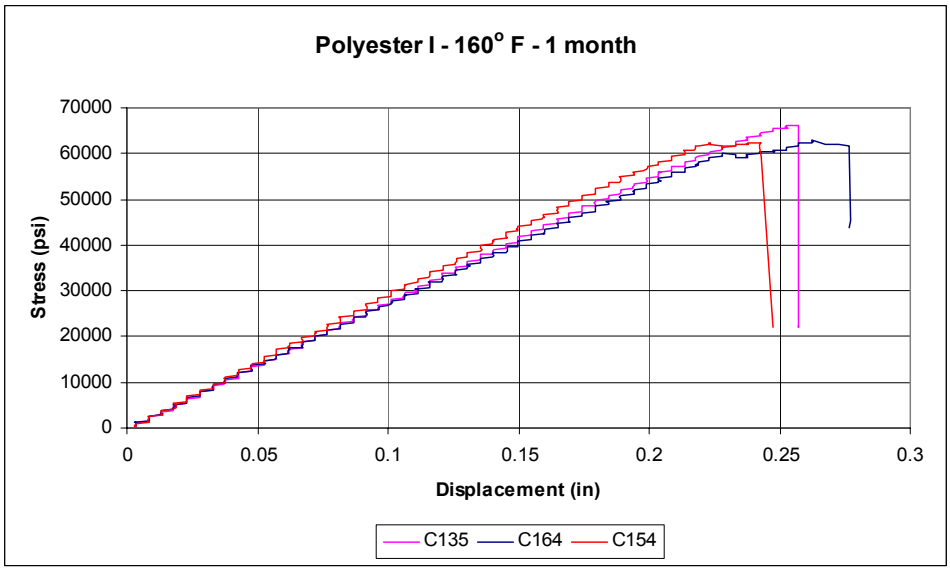

Figure C-22. Flexural test curves for Polyester I after 1 month at 160ºF.

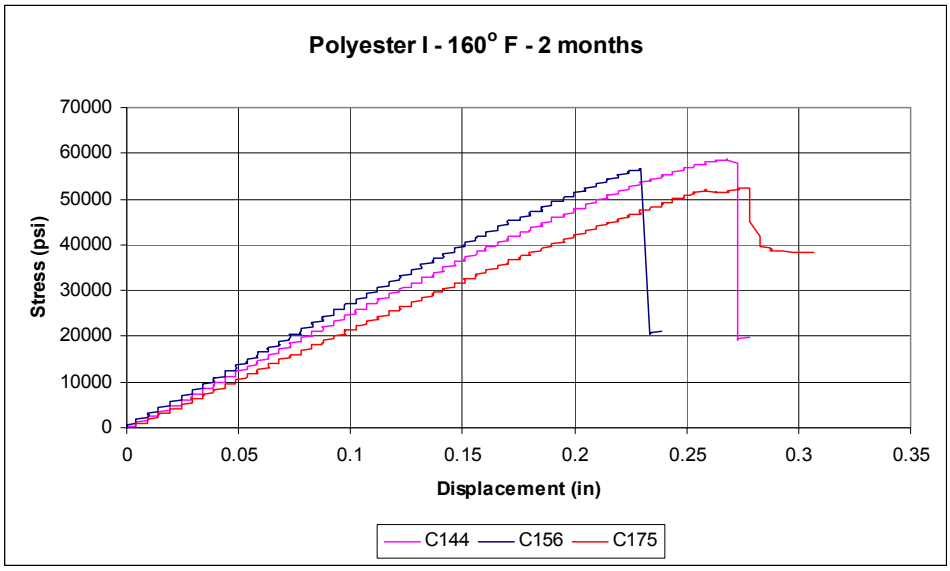

Figure C-23. Flexural test curves for Polyester I after 2 months at 160ºF.

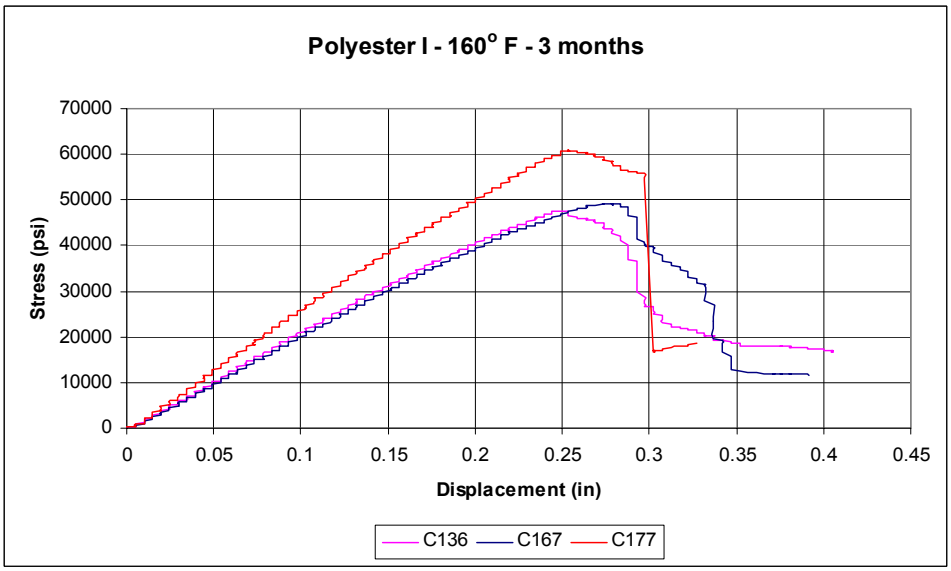

Figure C-24. Flexural test curves for Polyester I after 3 months at 160ºF.

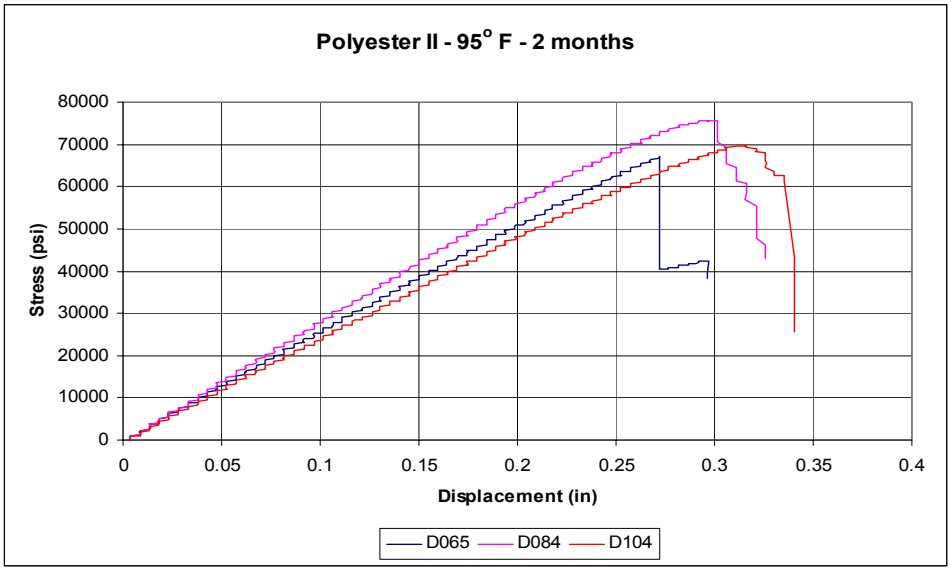

Figure C-25. Flexural test curves for Polyester II after 2 months at 95ºF.

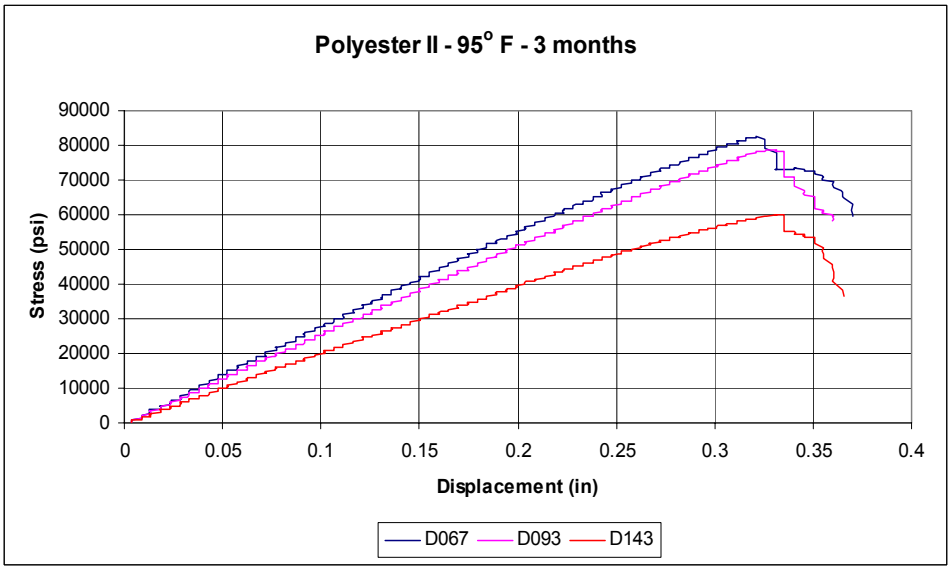

Figure C-26. Flexural test curves for Polyester II after 3 months at 95ºF.

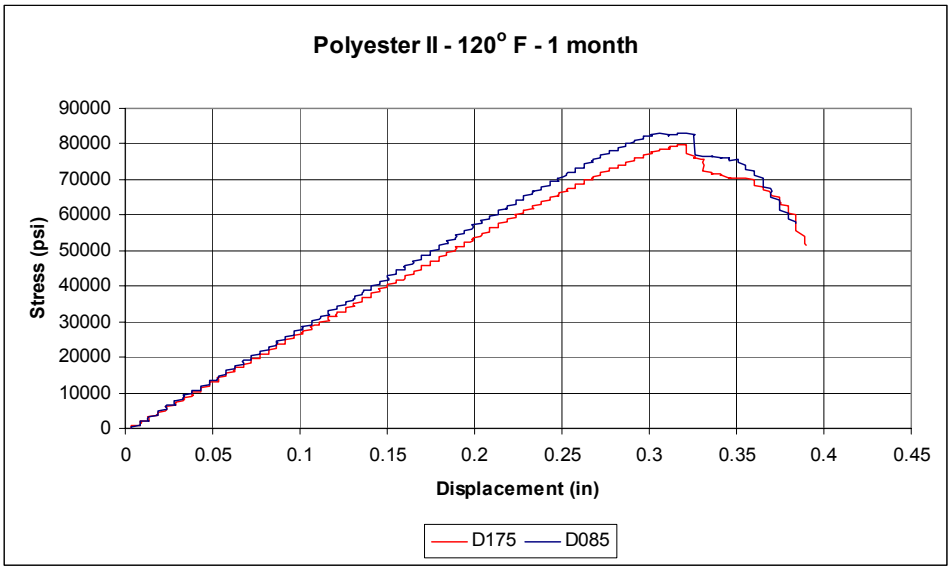

Figure C-27. Flexural test curves for Polyester II after 1 month at 120ºF.

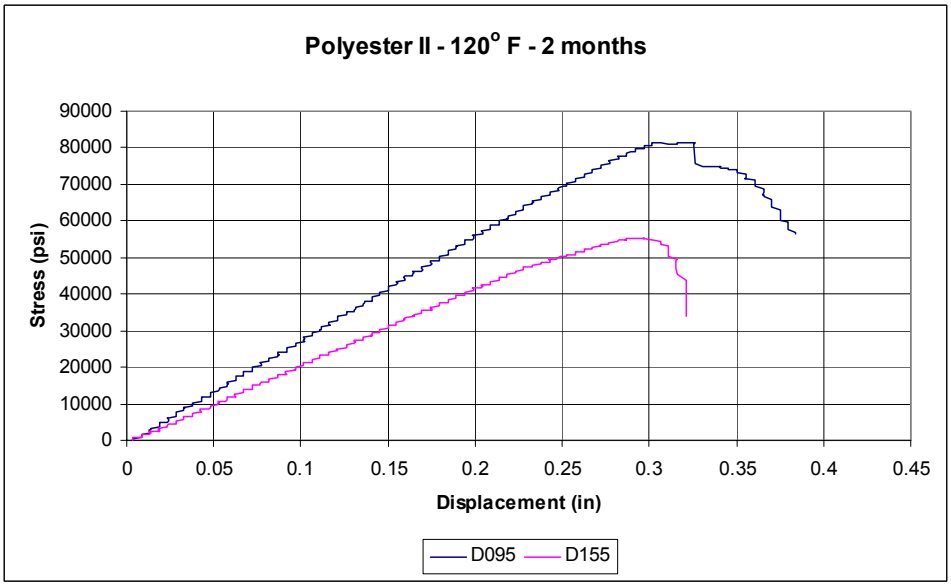

Figure C-28. Flexural test curves for Polyester II after 2 months at 120ºF.

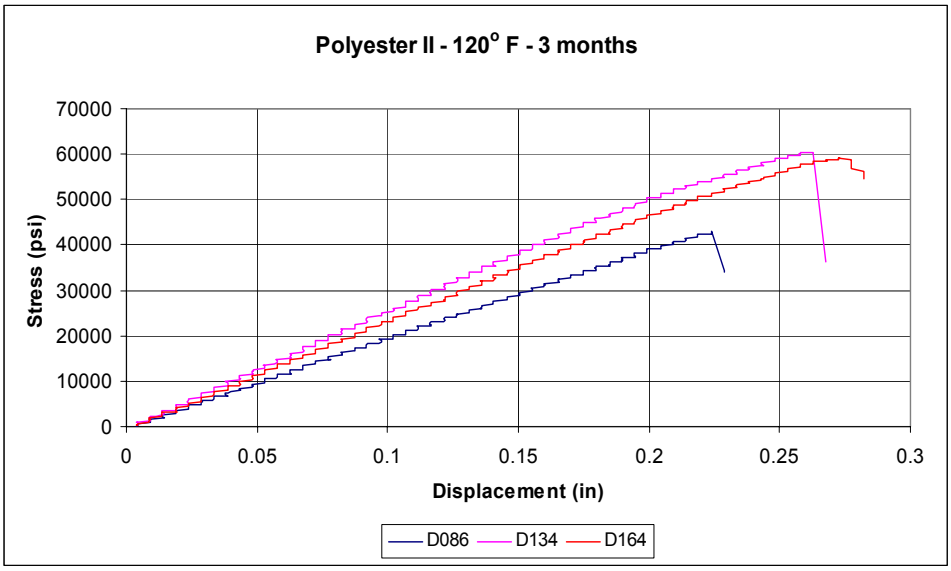

Figure C-29. Flexural test curves for Polyester II after 3 months at 120ºF.

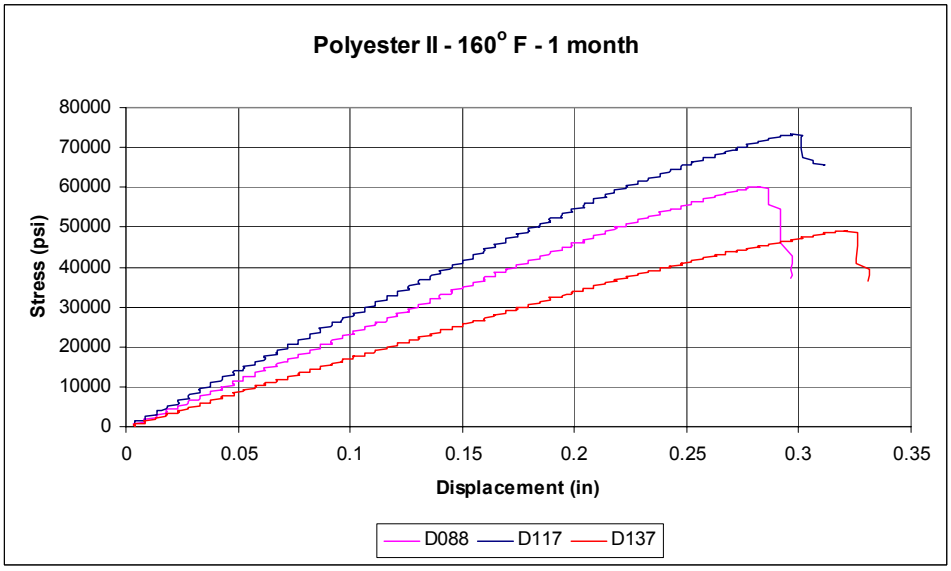

Figure C-30. Flexural test curves for Polyester II after 1 months at 160ºF.

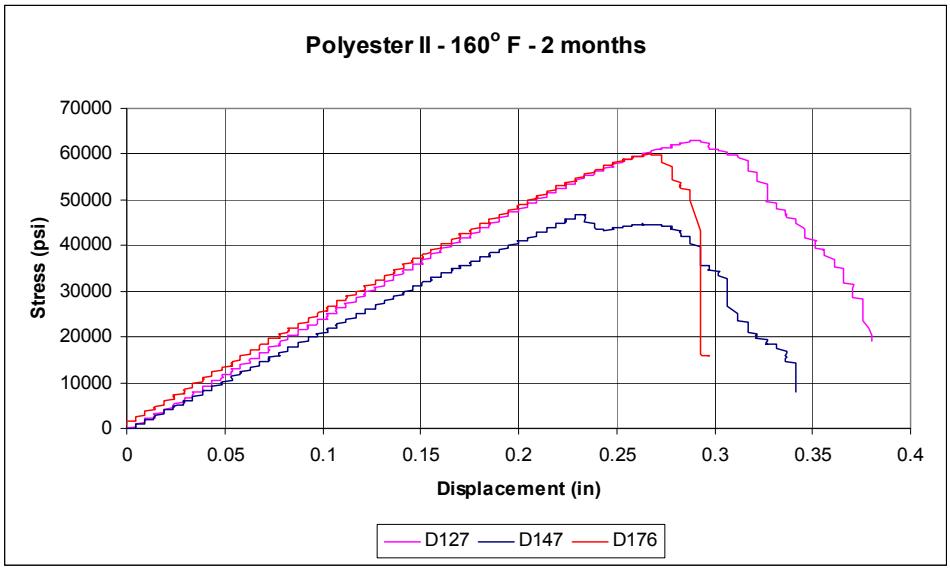

Figure C-31. Flexural test curves for Polyester II after 2 months at 160ºF.

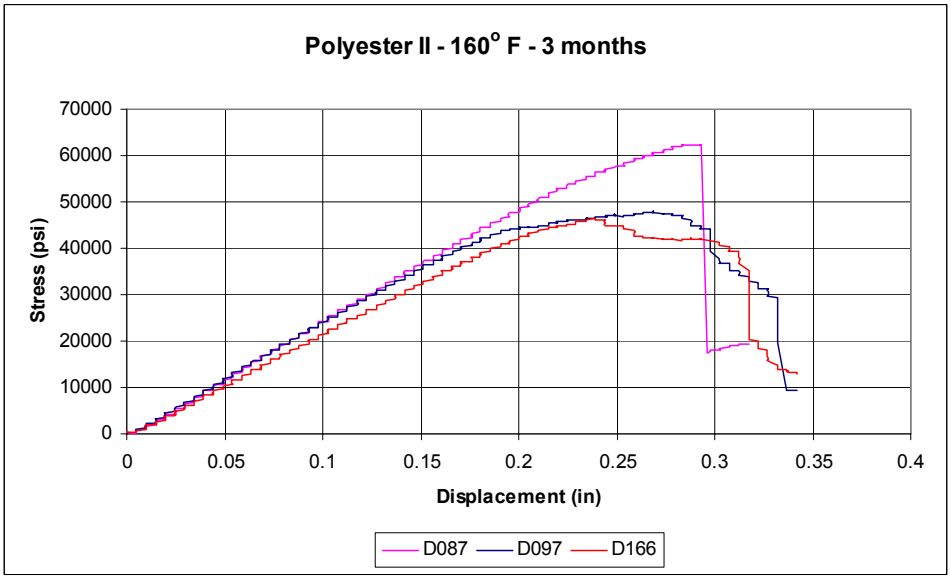

Figure C-32. Flexural test curves for Polyester II after 3 months at 160ºF.

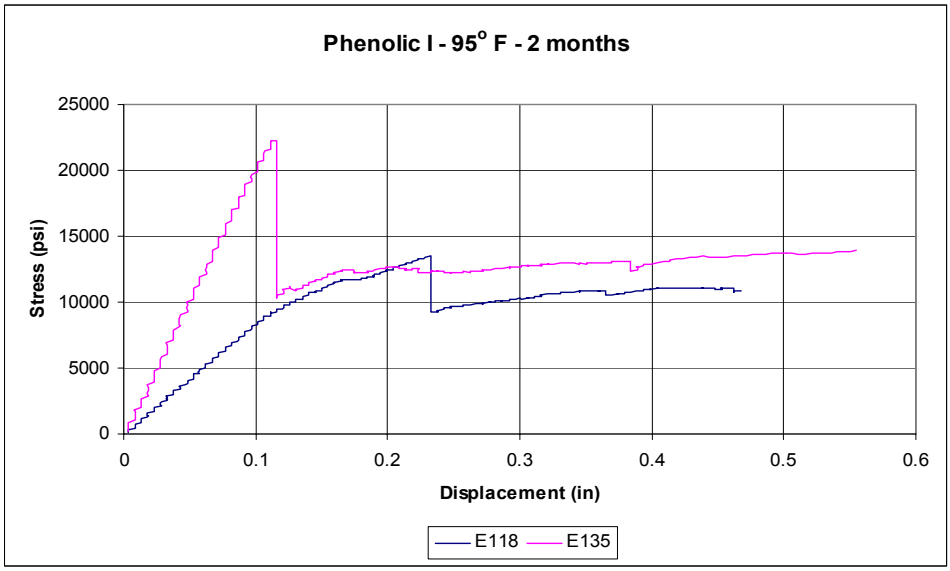

Figure C-33. Flexural test curves for phenolics after 2 months at 95ºF.

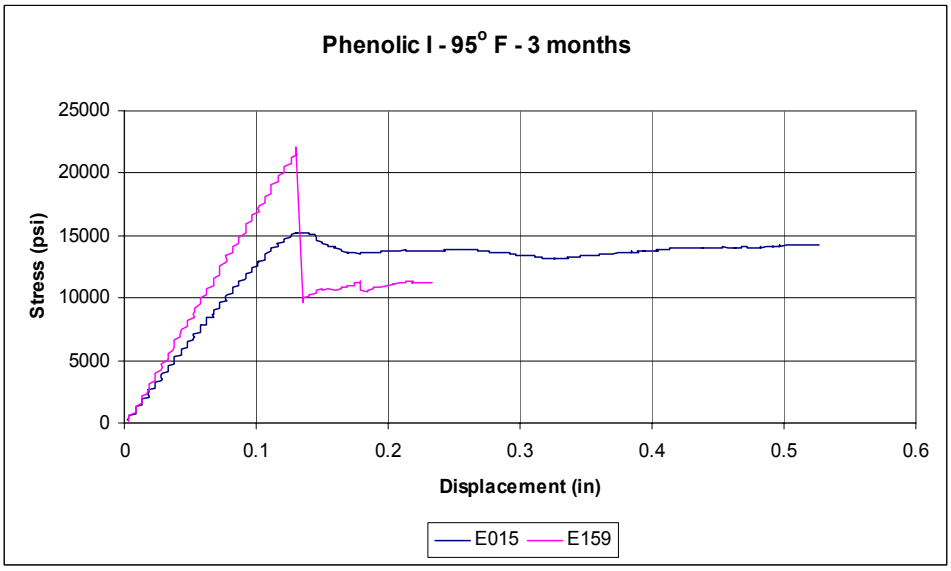

Figure C-34. Flexural test curves for phenolics after 3 months at 95ºF.

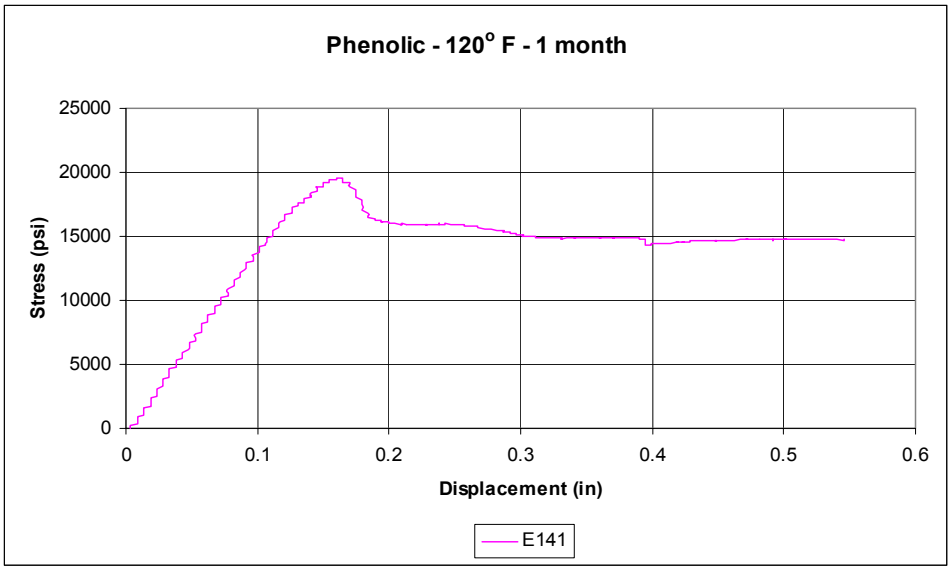

Figure C-35. Flexural test curves for phenolics after 1 month at 120ºF.

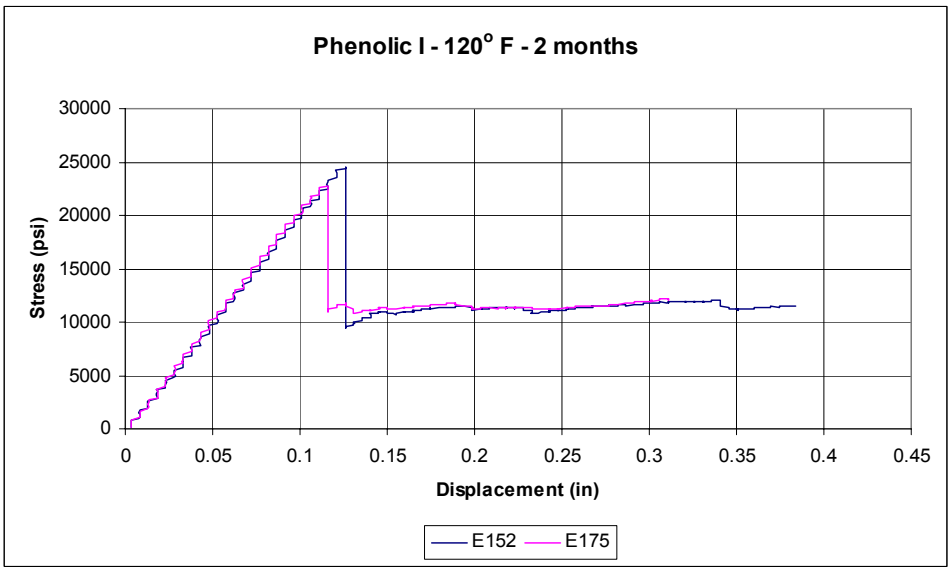

Figure C-36. Flexural test curves for Phenolic I after 2 months at 120ºF.

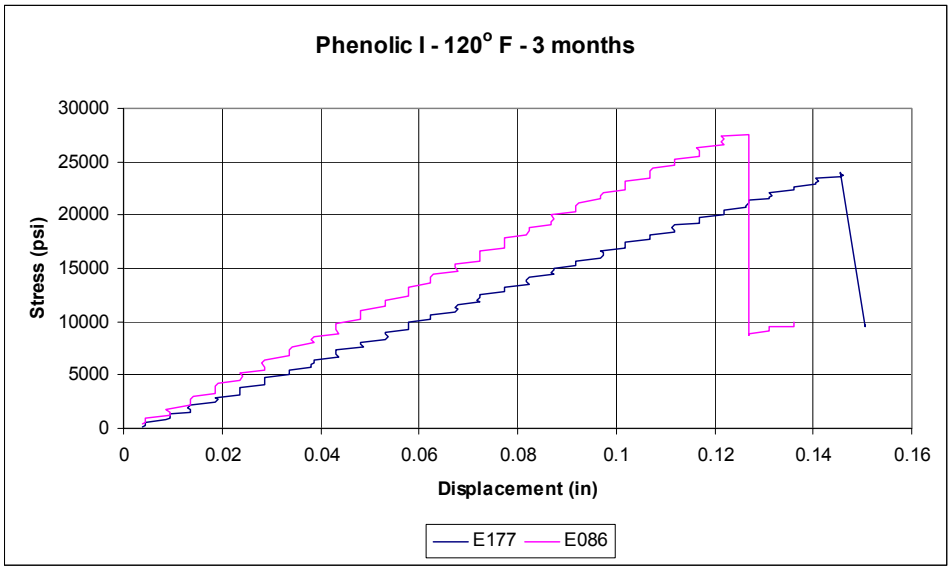

Figure C-37. Flexural test curves for phenolics after 3 months at 120ºF.

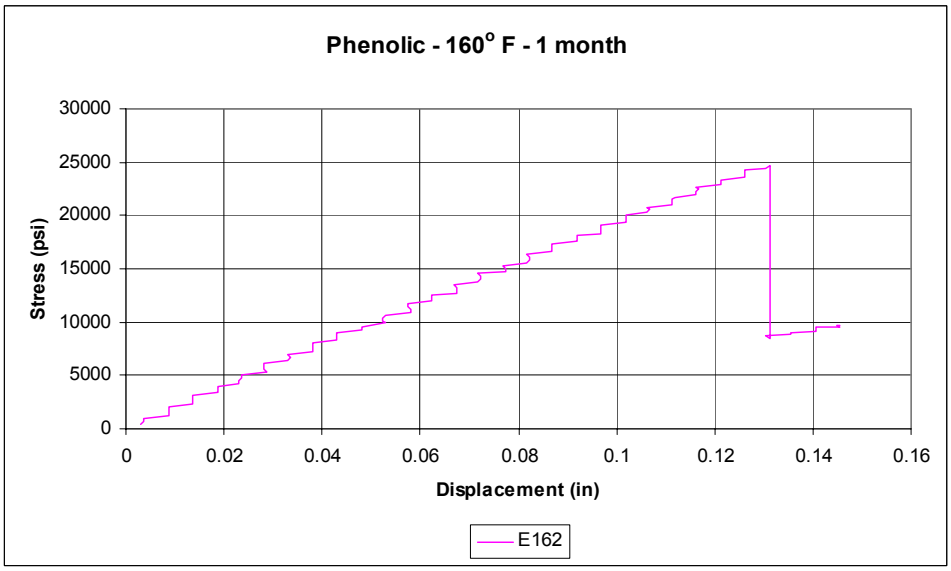

Figure C-38. Flexural test curves for phenolics after 1 months at 160ºF.

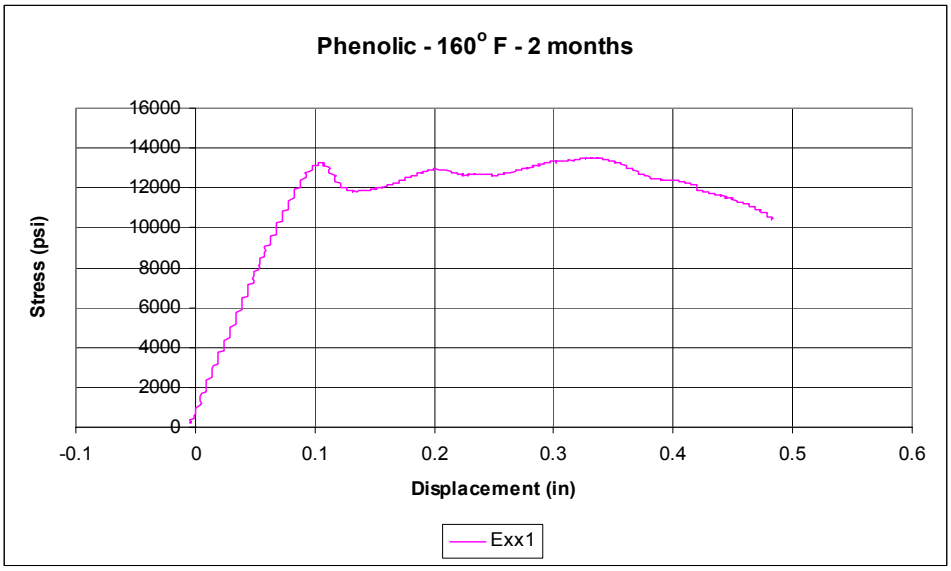

Figure C-39. Flexural test curves for phenolics after 2 months at 160ºF.

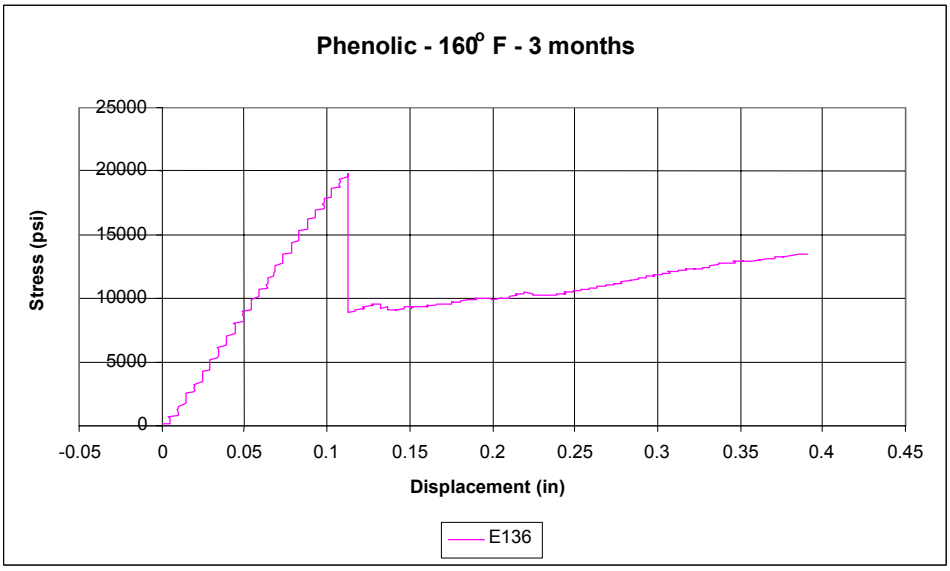

Figure C-40. Flexural test curves for phenolics after 3 months at 160ºF.

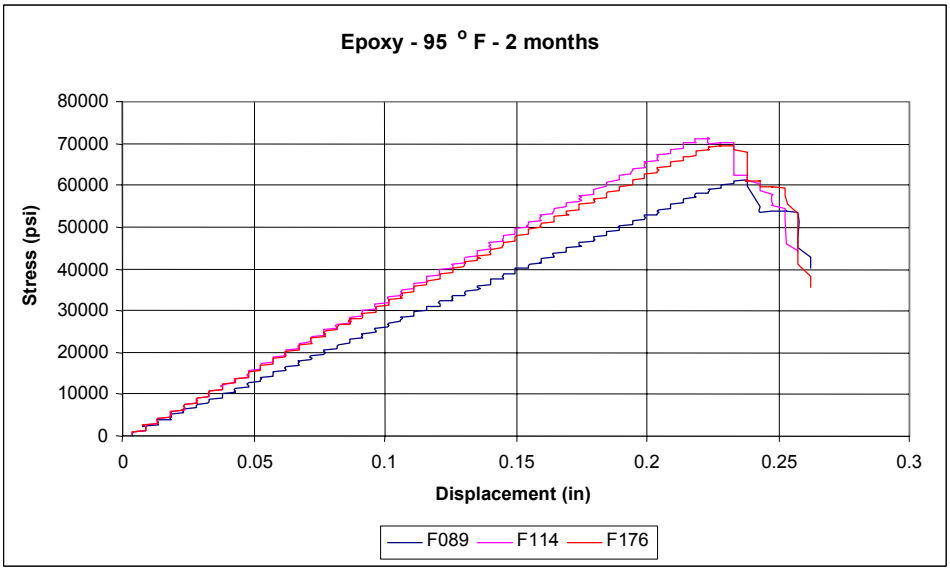

Figure C-41. Flexural test curves for epoxy after 2 months at 95ºF.

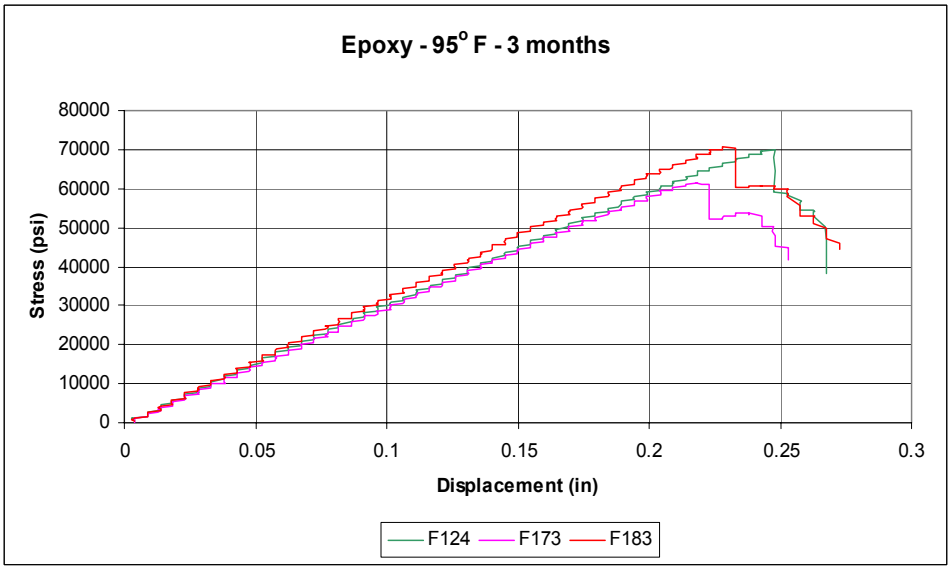

Figure C-42. Flexural test curves for epoxy after 3 months at 95ºF.

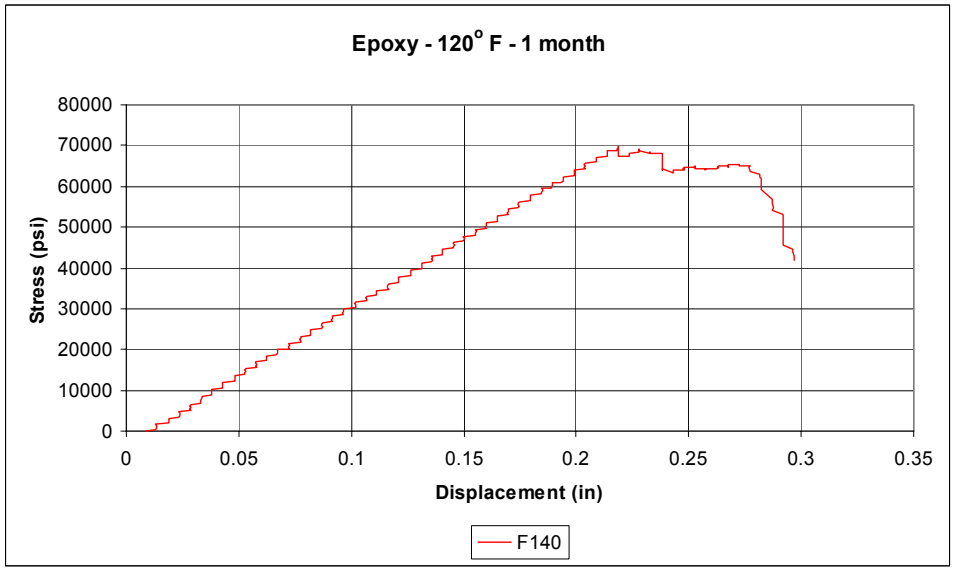

Figure C-43. Flexural test curves for epoxy after 1 month at 120ºF.

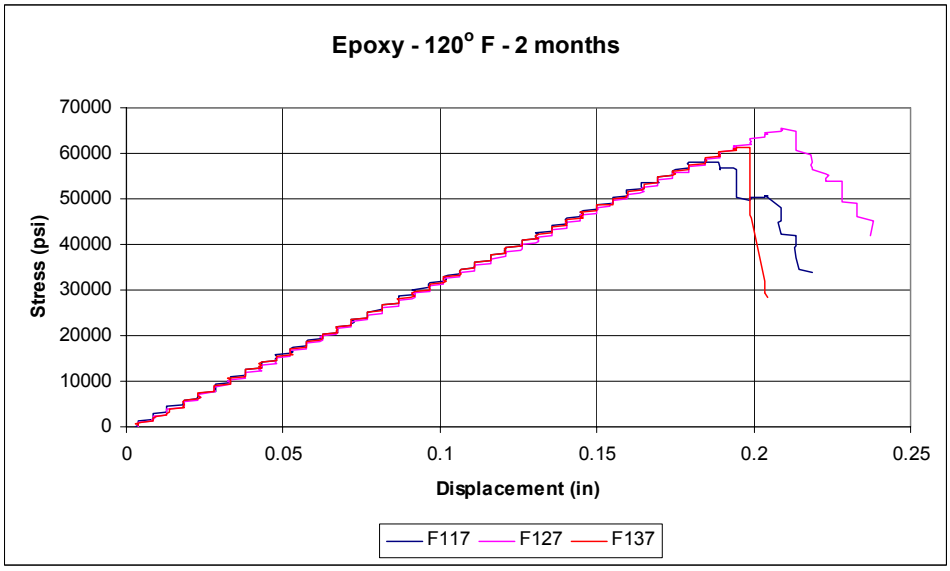

Figure C-44. Flexural test curves for epoxy after 2 months at 120ºF.

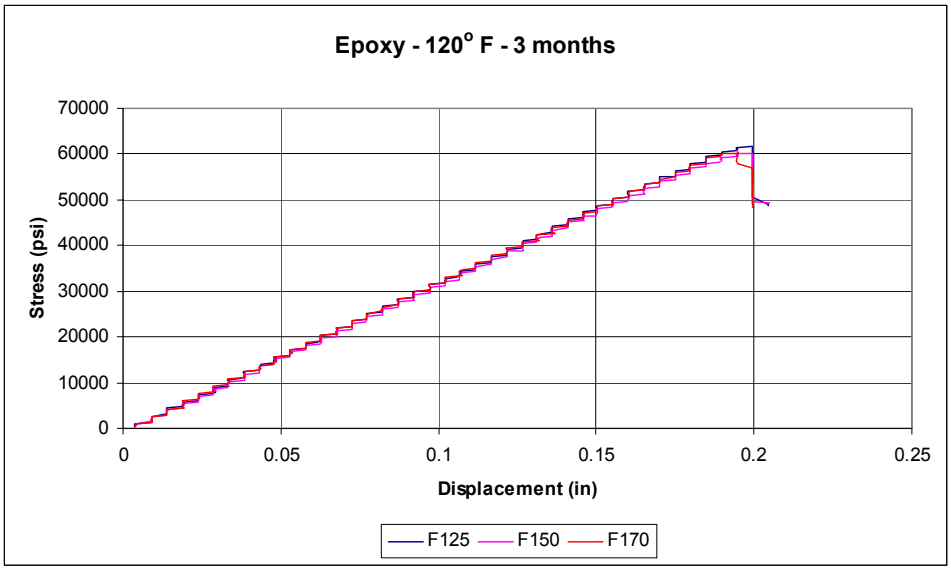

Figure C-45. Flexural test curves for epoxy after 3 months at 120ºF.

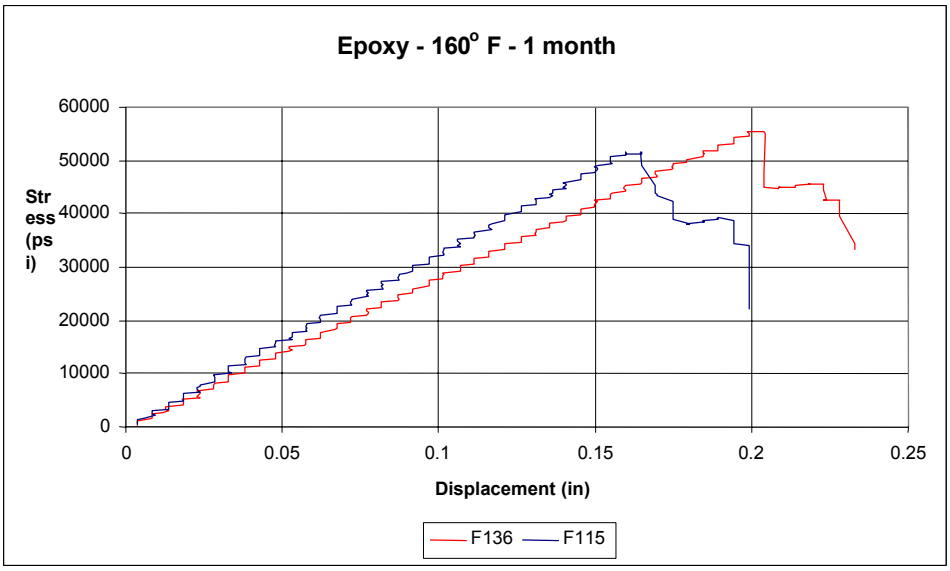

Figure C-46. Flexural test curves for epoxy after 1 month at 160ºF.

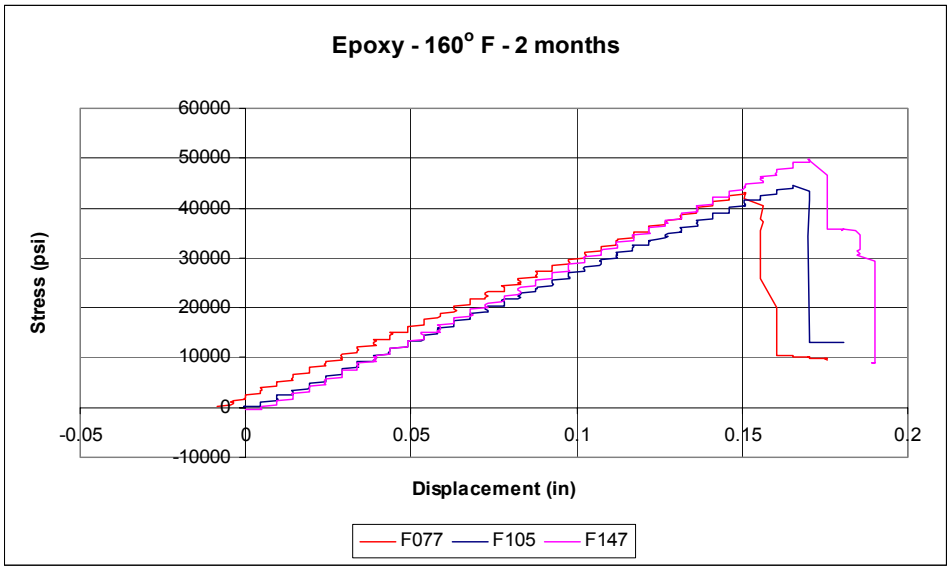

Figure C-47. Flexural test curves for epoxy after 2 months at 160ºF.

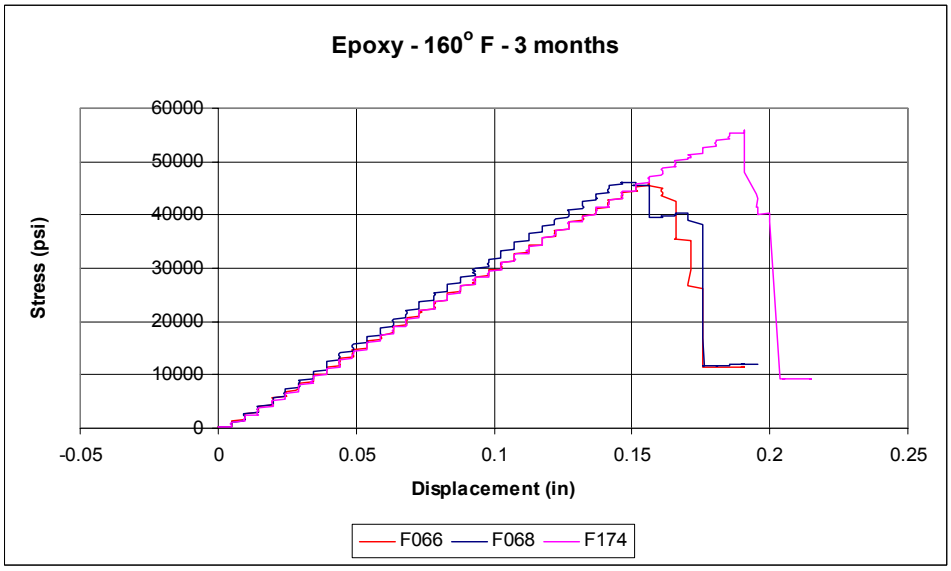

Figure C-48. Flexural test data for epoxy after 3 months at 160ºF.

Appendix D: Averaged DMA Curves of Exposed versus Control Flexural Storage and Loss Moduli

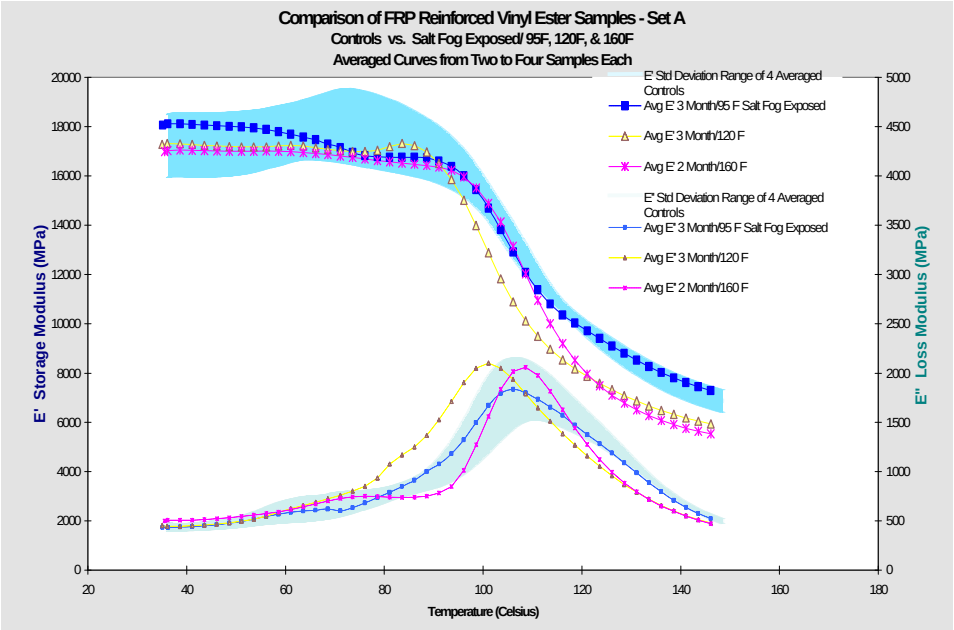

Figure D-1. Averaged DMA curves of exposed versus control flexural storage and loss moduli – Vinylester Samples Set A

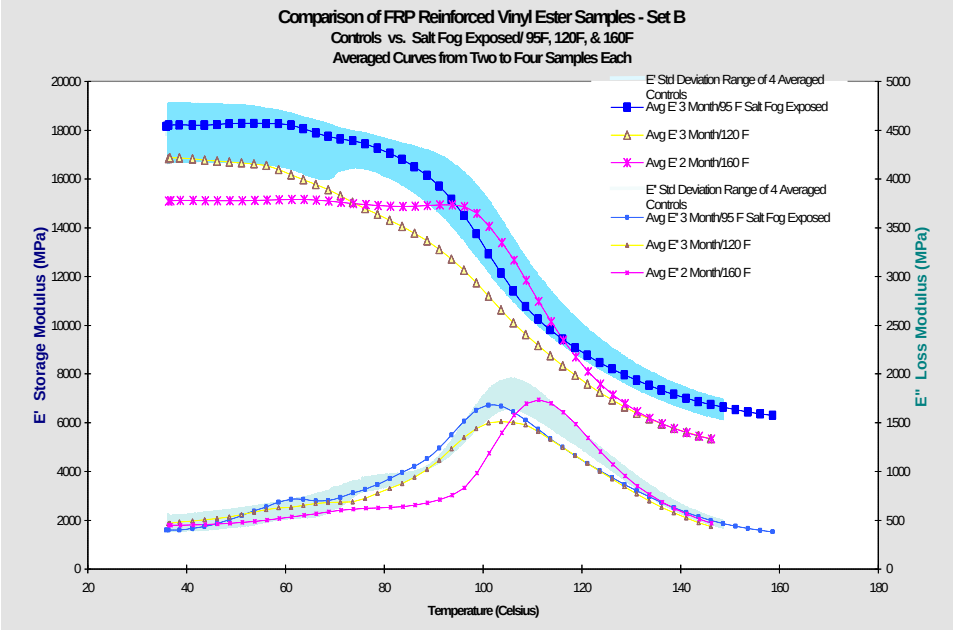

Figure D-2. Averaged DMA curves of exposed versus control flexural storage and loss moduli – Vinylester Samples Set B

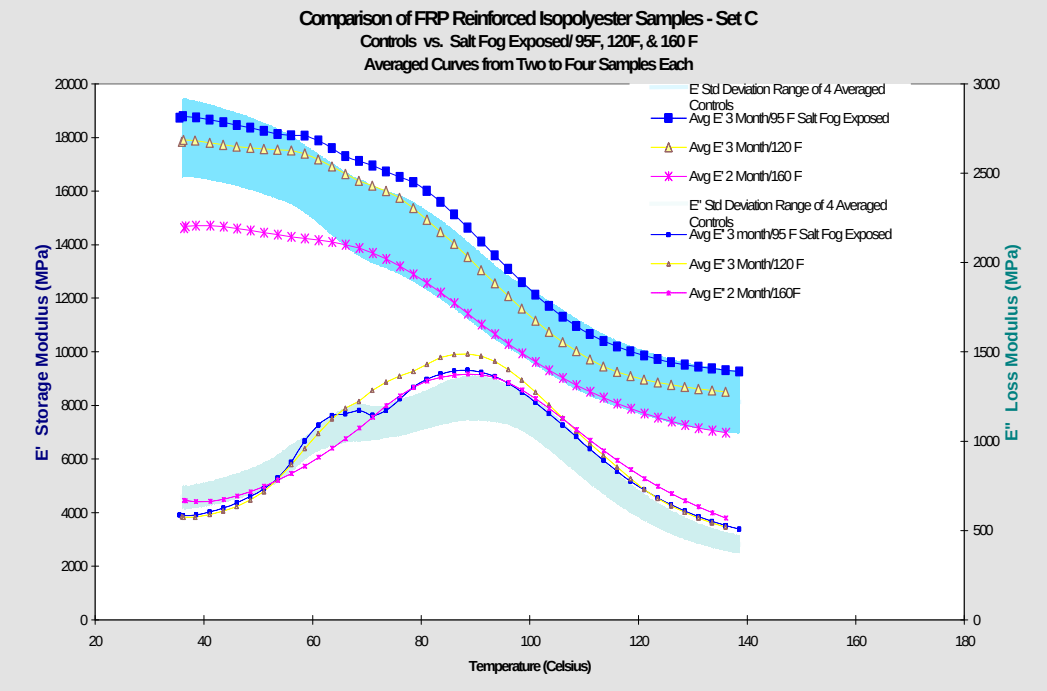

Figure D-3. Averaged DMA curves of exposed versus control flexural storage and loss moduli – Polyester Samples Set C

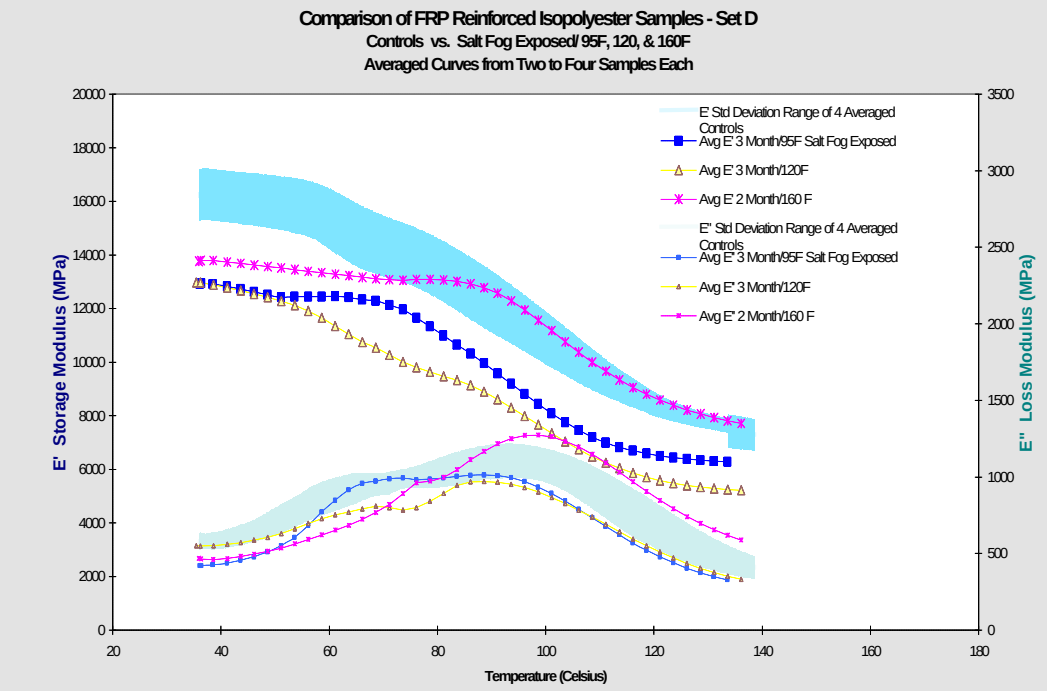

Figure D-4. Averaged DMA curves of exposed versus control flexural storage and loss moduli – Polyester Samples Set D

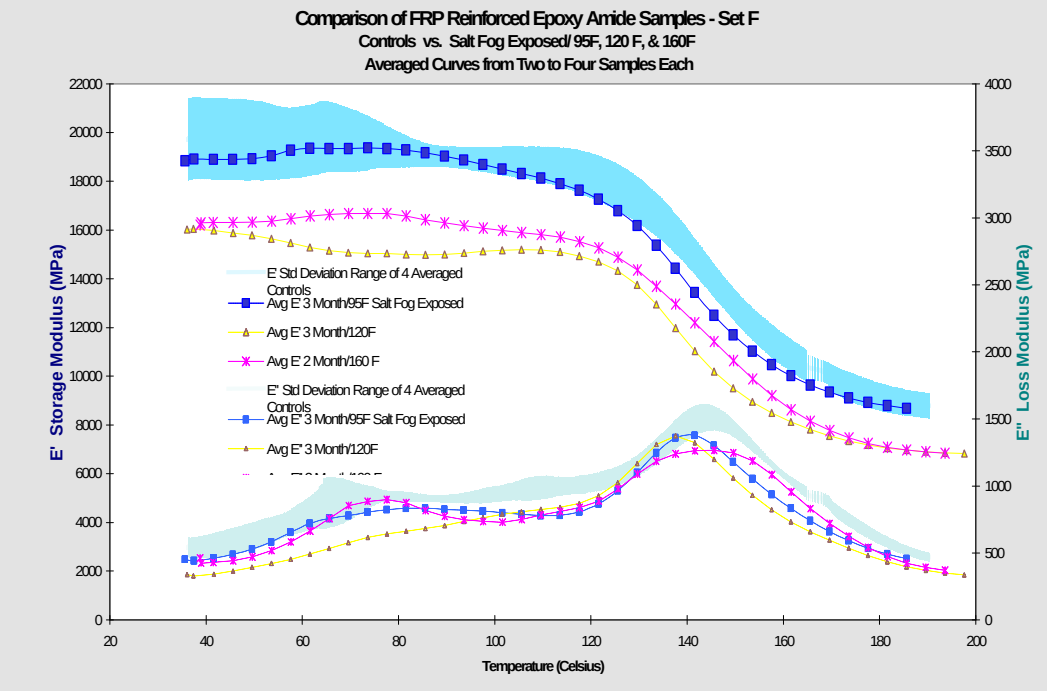

Figure D-5. Averaged DMA curves of exposed versus control flexural storage and loss moduli – Epoxy Amide Sample